HHS Public Access

Author manuscript

Nat Med. Author manuscript; available in PMC 2019 July 14.

Published in final edited form as:

Nat Med. 2019 March ; 25(3): 448–453. doi:10.1038/s41591-018-0324-z.

Healthy infants harbor intestinal bacteria that protect against food allergy

Taylor Feehley[#1], **Catherine H. Plunkett**[#1], **Riyue Bao**[#2,3], **Sung Min Choi Hong**[1], **Elliot Culleen**[1], **Pedro Belda-Ferre**[1], **Evelyn Campbell**[1], **Rosita Aitoro**[4], **Rita Nocerino**[4], **Lorella Paparo**[4], **Jorge Andrade**[2,3], **Dionysios A. Antonopoulos**[5], **Roberto Berni Canani**[4,6,7], and **Cathryn R. Nagler**[1,*]

[1]Department of Pathology and Committee on Immunology, The University of Chicago, Chicago, IL 60637, USA

[2]Center for Research Informatics, The University of Chicago, Chicago, IL 60637, USA

[3]Department of Pediatrics, The University of Chicago, Chicago, IL 60637, USA

[4]Department of Translational Medical Science, Section of Pediatrics, University of Naples, Federico II, Naples, Italy

[5]Department of Medicine, The University of Chicago, Chicago, IL 60637, USA and Biosciences Division, Argonne National Laboratory, Argonne, IL 60439, USA

[6]European Laboratory for the Investigation of Food-Induced Diseases, University of Naples, Federico II, Naples, Italy

[7]CEINGE Advanced Biotechnologies, University of Naples, Federico II, Naples, Italy

[#] These authors contributed equally to this work.

Abstract

There has been a striking generational increase in life-threatening food allergies in Westernized societies[1,2] One hypothesis to explain this rising prevalence is that 21[st] century lifestyle practices, including misuse of antibiotics, dietary changes, and higher rates of Caesarean birth and formula feeding have altered intestinal bacterial communities; early life alterations may be particularly detrimental.[3,4] To better understand how commensal bacteria regulate food allergy in humans we colonized germ free (GF) mice with feces from healthy or cow's milk allergic (CMA) infants [5]. We show here that GF mice colonized with bacteria from healthy, but not CMA, infants were protected against anaphylactic responses to a cow's milk allergen. Differences in bacterial

[*]To whom correspondence should be addressed; cnagler@bsd.uchicago.edu.

Author contributions

T.F., C.H.P, R.B. R.B.C. and C.R.N. designed the study. C.H.P. and T.F performed mouse experiments with help from P.B.F., R.A, E.C., E.C. and S.C.H. R.B., P.B.F and J.A. performed bioinformatics analysis. T.F., C.H.P., R.B., P.B.F. and C.R.N. analyzed results. R.B.C., R.N. and L.A. cared for patients and provided donor fecal samples. D.A.A. provided protocols and assisted with the colonization of GF mice with human feces and *A. caccae*. T.F., C.H.P., R.B., R.B.C. and C.R.N. wrote the manuscript. All authors read and commented on manuscript.

Author Information

C.R.N. is President and co-founder of ClostraBio, Inc. The other authors declare that they have no competing financial interests. Correspondence and requests for materials should be addressed to C.R.N. (cnagler@bsd.uchicago.edu).

composition separated the healthy and CMA populations in both the human donors and the colonized mice. Healthy and CMA colonized mice also exhibited unique transciptome signatures in the ileal epithelium. Correlation of ileal bacteria with genes upregulated in the ileum of healthy or CMA colonized mice identified a Clostridial species, *Anaerostipes caccae*, that protected against an allergic response to food. Our findings demonstrate that intestinal bacteria are critical for regulating allergic responses to dietary antigens and suggest that interventions that modulate bacterial communities may be therapeutically relevant for food allergy.

Work from our laboratory, and others, has demonstrated that the fecal microbial communities of infants with cow's milk allergy (CMA) are markedly different from their healthy counterparts [5,6]. Based on these results, as well as evidence that members of the microbiota can be allergy-protective [7], we used a gnotobiotic mouse model to investigate whether commensal bacteria play a causal role in protection against an allergic response to the cow's milk allergen β-lactoglobulin (BLG). Germ free (GF) mice were colonized with human feces from four healthy and four IgE-mediated CMA infant donors who were matched for age, gender and mode of birth [8,9] (Supplementary Table 1). It has previously been reported that diet plays an important role in the stable colonization of GF mice with human feces [10]. To support the growth of human bacteria in the murine hosts, mice received feces from formula-fed healthy or CMA infants and were fed the same formulas consumed by their human infant donors in addition to plant-based mouse chow. The CMA infant donors received an extensively hydrolyzed casein formula (EHCF) to manage ongoing allergic symptoms while the healthy donors received a standard cow's milk-based formula [5]. Initial transfer recipients were used as living repositories for subsequent experiments (see Methods).

Groups of GF mice and mice colonized with either the healthy or CMA infant microbiota were sensitized with BLG and the mucosal adjuvant cholera toxin (CT). Consistent with previous reports[7,11], GF mice, devoid of any bacterial colonization, were highly susceptible to anaphylactic responses to food as evidenced by a drop in core body temperature (Fig. 1a) and production of BLG-specific IgE and IgG1 (Fig. 1b, c). We also measured a substantial reduction in core body temperature in mice colonized with fecal samples from each of the four CMA donors in response to BLG challenge (Fig. 1a). Sensitized CMA-colonized mice produced significantly higher serum concentrations of BLG-specific IgE (Fig. 1b), IgG1 (Fig. 1c) and mMCPT-1 (Fig. 1d) when compared to healthy-colonized mice. Strikingly, all of the mice that received the four healthy infant microbiotas were protected from an anaphylactic response to BLG challenge; their core body temperature post-challenge was significantly different from that measured in GF or CMA-colonized mice (Fig. 1a). Histological analysis did not reveal any evidence of pathology or inflammation in ileal or colonic tissue samples taken post-challenge (Extended Data Fig. 1) or after long term colonization (Extended Data Fig. 2). Microbial analysis revealed that community diversity and evenness were similar between healthy and CMA colonized mouse groups (Extended Data Fig. 3). To examine whether the cow's milk containing formula contributed to microbiota-independent protection against anaphylaxis in the healthy-colonized mice, we performed additional fecal transfers from breast-fed healthy and CMA donors (Supplementary Table 2). Recipient mice received only plant-based mouse chow. Mice

colonized with feces from the breast-fed healthy donor were protected from an anaphylactic response to BLG sensitization and challenge. However, mice colonized with feces from a breast-fed CMA donor exhibited a significantly greater drop in core body temperature compared to healthy-colonized mice (Extended Data Fig. 4a) and higher levels of BLG specific IgE (Extended Data Fig. 4b). We also compared sensitization to BLG in GF mice fed water or Enfamil. Both groups of mice responded robustly to sensitization with BLG (Extended Data Fig. 5). There was no significant difference in their drop in core body temperature post challenge or in serum concentrations of BLG-specific IgE or IgG1; serum mMCPT-1 was, however, suppressed in mice fed the cow's milk containing formula.

Analysis of fecal samples from the eight formula-fed human infant donors (Supplementary Table 1) identified 58 OTUs that were differentially abundant between healthy and CMA infants (Fig. 2a; Supplementary Table 3). Since variation exists between each donor and murine transfer recipient at the single OTU level, we examined whether donor-derived microbiome composition differences were able to distinguish the colonized mouse groups. As an aggregated measure to present the data, we calculated the number of potentially "protective" (more abundant in healthy donors, n=34) and potentially "non-protective" (more abundant in CMA donors, n=24) OTUs to produce a presence/absence ratio for each donor (Extended Data Fig. 6a; see Methods). In addition, we calculated a score weighted toward each OTU based on its relative abundance in the sample (hereafter called abundance score) (Fig. 2a; see Methods). When the OTU abundance score was plotted against the presence/absence ratio, donors segregated by ratio into the healthy and CMA groups (Extended Data Fig. 6b, **squares**). This threshold also separated the CMA- and healthy-colonized mice by their biological phenotype (Extended Data Fig. 6b, **circles**), demonstrating that this donor-derived aggregated microbiota signature is validated in the murine transfer recipients. The significantly higher protective/non-protective OTU ratio in healthy infants relative to those with CMA was independently corroborated in an unrelated set of samples from the same Neapolitan cohort by reanalysis of 16S fecal sample data collected in a previously published study[5] (Extended Data Fig. 7).The donor-derived OTU ratio also separated healthy- and CMA-colonized mice when plotted against biomarkers of allergic disease including BLG-specific IgE (Fig. 2b), BLG-specific IgG1 (Fig. 2c) and mMCPT-1 (Fig. 2d). Interestingly, linear discriminant effect size (LEfSe) analysis (Fig. 2e, f) showed that *Lachnospiraceae*, a family in the Clostridia class, previously implicated in protection against allergic sensitization to food, were enriched in the healthy colonized mice [7].

Tolerance to dietary antigens begins with their absorption in the small intestine [4,12]. Most commensal bacteria reside in the colon; in the small intestine, bacteria are most numerous in the ileum [13]. The interaction of these bacteria with IECs is central to regulation of immunity at the host-microbe interface [13,14]. We therefore isolated ileal IECs from groups of mice colonized by each of the eight infant donors and quantified gene expression by RNASeq (Fig. 3a). We found that healthy-colonized mice upregulated a unique set of ileal genes compared to CMA-colonized mice (Fig. 3a; Supplementary Table 4). For example, *Fbp1*, which encodes a key gluconeogenic enzyme abundantly expressed in epithelial cells of the small intestine[15], was significantly upregulated across all healthy-colonized mice (Fig. 3a).

Reduced expression of *Fbp1* has been associated with a metabolic switch from oxidative phosphorylation to aerobic glycolysis [16,17] which alters oxygenation of the epithelium and contributes to dysbiosis [18]. *Tgfbr3* and *Ror2* were downregulated in the ileum of CMA-colonized mice relative to healthy-colonized mice (Fig. 3a). *Tgfbr3* encodes a receptor for the growth factor TGF-β and is abundantly expressed in the small intestine of suckling rats [19]. Soluble TGFβRIII and TGF-β2 are present at high concentrations in breast milk; activation of TGF-β signaling by Wnt5a is mediated through *Ror2* and is important for epithelial repair [20]. By contrast, *Acot12* and *Me1*, genes involved in pyruvate metabolism, were upregulated in the ileum of CMA-colonized mice relative to healthy-colonized mice. These metabolic and molecular processes are reflected in the Gene Ontology pathways significantly altered in CMA- and healthy-colonized mice depicted in Fig. 3b.

To determine whether the fecal OTU signatures identified in Fig. 2 are also reflective of ileal bacterial populations we examined the correlation between ileal OTUs and the fecal signature in healthy- and CMA-colonized mice (Extended Data Fig. 8a). We found that the majority of the taxa change in the same direction (increase or decrease in abundance) in healthy relative to CMA between mouse fecal and ileal samples (Extended Data Fig. 8b, c). The identification of differential gene expression in ileal IECs from healthy- and CMA-colonized mice (Fig. 3a) suggested that ileal bacteria regulate host immunity to contribute to allergic sensitization. Integrative analysis of ileal bacteria and ileal differentially expressed genes (DEGs) revealed 9 OTUs significantly and consistently correlated with genes upregulated in the ileum of healthy- or CMA-colonized mice (Fig. 4a). Interestingly, 3/5 of the protective OTUs associated with DEGs upregulated in the ileum of healthy colonized mice are members of the family *Lachnospiraceae*; 70% of the OTUs in our previously identified allergy protective murine Clostridia consortium belong to this family [7]. A BLAST search of assembled 16S sequences against the NCBI database (16S ribosomal RNA, Bacteria and Archaea) revealed that all three protective *Lachnospiraceae* OTUs upregulated in the healthy colonized mice (259772, New18, 177986) have *Anaerostipes caccae* as the closest matching species. In particular, OTU259772 was annotated with *A. caccae* in a previous study of human infant feces and diet [21]. *A. caccae* is non-spore forming, utilizes lactate and acetate and produces butyrate [22,23]. Spearman's correlation between *Lachnospiraceae* OTU259772 and several highly correlated ileal DEGs of interest (*Ror2, Fbp1, Tgfbr3, Acot12* and *Me1)* from Fig. 3a are depicted in Fig. 4b. Analysis of ileal and fecal samples using quantitative PCR (qPCR) with previously validated species-specific primers [24] provided independent confirmation of the enrichment of *A. caccae* in healthy-colonized mice (Fig. 4c-e and Extended Data Fig. 9a-c). Abundance of *A. caccae* in ileal samples also correlated with DEGs from ileal IECs (Extended Data Fig. 10). Of note, two of the highly correlated DEGs (*Acot12* and *Me1)* are involved in pyruvate metabolism. Butyrate is an important energy source for colonic epithelial cells [25]. Butyrate drives oxygen consumption by colonocytes through β-oxidation, thereby maintaining a locally hypoxic niche for butyrate-producing obligate anaerobes[26]. Under conditions of dysbiosis, colonocytes generate energy via glycolysis, a process that includes production of pyruvate as a key intermediate[27]. It is tempting to speculate that the negative correlation between the abundance of butyrate-producing *A. caccae* and pyruvate metabolism-related genes in IECs

from CMA-colonized mice is reflective of metabolic shifts in ileal epithelial function under conditions of dysbiosis.

We next examined whether *A. caccae* can mimic the changes in gene expression and protection against anaphylaxis associated with the healthy microbiota by monocolonizing GF mice (see Methods). Some of the genes significantly upregulated in healthy-colonized mice (*Fbp1, Tgfbr3*) were also significantly upregulated in *A. caccae* monocolonized mice (Fig. 4f) when compared to GF or CMA-colonized mice. *Acot12* expression was significantly upregulated in CMA-colonized mice, but not in healthy-colonized or *A. caccae* monocolonized mice (Fig. 4f). BLG + CT sensitized *A. caccae* monocolonized mice were protected against an anaphylactic response to BLG challenge. As in Fig. 1, CMA colonized mice exhibited a marked drop in core body temperature indicative of anaphylaxis (Fig. 4g). Both the changes in core body temperature and serum concentrations of mMCPT-1 were significantly reduced in *A caccae* monocolonized mice compared to CMA colonized mice (Fig. 4 g, j). Antigen specific, Th2 dependent, antibody (serum BLG-specific IgE and IgG1) (Fig. 4 h, i) and cytokine responses IL-13 and IL-4 (Fig. 4 k, l) were all reduced in *A caccae* monocolonized mice.

Anaerobic, mucosa-associated bacteria in the Clostridia class have attracted considerable interest because of their reported roles in the maintenance of intestinal homeostasis through induction of regulatory T cells [28,29], production of immunomodulatory metabolites [30,31] and regulation of colonization resistance [32]. Previous studies have focused mostly on the colon. We now also place these immunomodulatory bacteria in the ileum, at the site of food absorption and demonstrate their causal role in protection against an anaphylactic response to food. Mechanistic analysis of the Clostridia-associated changes in ileal gene expression described herein is likely to reveal additional pathways critical to the maintenance of tolerance to dietary antigens. The model described in this report does not address whether the allergic state drives dysbiosis [33] or dysbiosis precedes allergy. Indeed, many factors are likely to contribute to the development of food allergies. Our data demonstrate that the commensal bacteria play an important role in preventing allergic responses to food and provides proof of concept for the development of microbiome-modulating strategies to prevent or treat this disease.

Methods

Gnotobiotic Mouse Husbandry.

All mice were bred and housed in the Gnotobiotic Research Animal Facility (GRAF) at the University of Chicago. GRAF is an operational facility of the University of Chicago Animal Resource Center. Mice were maintained in Trexler style flexible film isolator housing units (Class Biologically Clean) with Ancare polycarbonate mouse cages (catalog #N10HT) and Teklad Pine Shavings (7088; sterilized by autoclave) on a 12-hour light/dark cycle at a room temperature of 20-24°C. Mice were provided with autoclaved sterile water, USP grade, at pH 5.2 *ad libitum*. Bedding was changed weekly; cages of formula fed mice required near daily bedding changes due to leakage of formula from the bottles. All mice were fed Purina Lab Diet® 5K67, stored in a temperature-controlled environment in accordance with The Guide for the Care and Use of Laboratory Animals (8th Edition, 2013). The diet was

sterilized by autoclaving at 121°C × 30 minutes. The sterility of the isolators was checked weekly by both cultivation and 16S rRNA analysis of fecal samples by qPCR. Cultivation was in BHI, Nutrient and Sabbaroud Broth at 37°C aerobic and anaerobic and 42°C aerobic for 96 hours. All mice are initially screened upon rederivation or receipt for all internal and external parasites, full serology profile and/or PCR, bacteriology, and gross and histologic analysis of major organs through either IDEXX Radil or Charles River Lab using an Axenic Profile Screen. Germ free (GF) C3H/HeN mice were transferred within the facility from T. Golovkina (University of Chicago).

Preparation of human fecal samples.

Healthy (non-allergic) fecal samples were obtained from participants in a vaccination program. These subjects were not at risk for atopic disorders and their clinical history was negative for any allergic condition. Infants with CMA were diagnosed at a tertiary pediatric allergy center (Pediatric Allergy Program at the Department of Translational Medical Science of the University of Naples 'Federico II'); for complete patient information see Supplementary Tables 1 and 2. All aspects of this study were conducted in accordance with the Declaration of Helsinki and approved by the Ethics Committee of the University of Naples 'Federico II'. Written informed consent was obtained from the parents/guardians of all children involved in the research. Fresh fecal samples were collected in the clinic in sterile tubes, weighed, mixed with 2mL LB broth+30% glycerol per 100-500mg, aliquoted into sterile cryovials and immediately stored at −80°C. Samples were shipped to the University of Chicago on dry ice where they were stored at −80°C until homogenization. To colonize mice, frozen fecal samples were introduced into an anaerobic chamber and thawed. Thawed feces were mixed with 3mm borosilicate glass beads in a sterile 50mL tube with 2.5mL pre-reduced PBS+0.05% cysteine and vortexed gently to dissociate. The resulting homogenate was filtered through a 100μm filter. This homogenization and filtration process was repeated three more times and the final filtrate was mixed with an equal volume of 30% glycerol+0.05% cysteine. This solution was aliquoted into Balch tubes with rubber stoppers for transport and introduction into the gnotobiotic isolator. The remaining fecal solution was frozen in aliquots at −80°C.

Colonization of germ free mice.

All mice were weaned at 3 weeks of age onto a plant-based mouse chow (Purina Lab Diet® 5K67) and colonized at weaning. GF mice received autoclaved sterile water. Both male and female mice were used for all experiments. Each experiment was littermate controlled. All mice were identified by unique 5 digit ear tags. All work was performed in accordance with the University of Chicago Institutional Biosafety and Animal Care and Use Committees. Each human infant donor transfer was maintained in its own flexible film isolator to avoid cross contamination. In all experiments, repository mice were created from human fecal donors by intragastric gavage of GF mice with 500μL of freshly prepared infant fecal homogenate. These repositories were then used to colonize subsequent experimental mice via mouse to mouse transfer by intragastric gavage of mouse feces. Fecal samples from both repository and experimental mice were examined regularly by 16S rRNA analysis which demonstrated that mouse to mouse transfer from repository to experimental mice by gavage was highly reproducible and stable over time. For colonization of experimental mice, a

freshly voided fecal pellet from a repository mouse was homogenized in 1mL of sterile PBS and 250μL of this homogenate was used to gavage one recipient mouse. For mice fed infant formula, the drinking water was replaced by formula four hours prior to colonization. Mice colonized with healthy infant feces were given Enfamil Infant (Mead Johnson Nutrition, Evansville, IN) and CMA-colonized mice were given extensively hydrolyzed casein formula (EHCF), Nutramigen I (Mead Johnson Nutrition) *ad libitum*. Both dry and liquid forms of the formulas were utilized. Dry formula was mixed with autoclaved sterile water, USP grade, according to the manufacturer's instructions. All formulas were refreshed daily.

For *Anaerostipes caccae* monocolonized mice, *A. caccae* (DSM-14662, DSMZ) was cultured in an anaerobic chamber (Coy, Model B) in reduced Schaedler's Broth (Remel) overnight at 37°C to an optical density (OD600) of 1.08. 250μL (approximately 2.5×10^8 CFU) was gavaged to GF mice. These mice were monitored for colonization by qPCR and were maintained as living repositories. For colonization of experimental mice, Enfamil Infant formula (liquid) was added to the drinking water four hours prior to colonization. A freshly voided fecal pellet from a repository mouse was then homogenized in 1mL of sterile PBS and 250μL of this homogenate was used to gavage one recipient mouse. Monocolonization with *A. caccae* was confirmed by qPCR with species-specific primers (Supplementary Table 6).

16S rRNA-targeted sequencing.

Bacterial DNA was extracted using the Power Soil DNA Isolation Kit (MoBio). 16S rRNA gene amplicon sequencing was performed on an Illumina MiSeq at the Environmental Sample Preparation and Sequencing Facility at Argonne National Laboratory. Procedures described in ref. [34] were used to generate 151bp paired-end reads from the fecal samples with 12 bp barcodes. The V4 region of the 16S rRNA gene was PCR amplified with region-specific primers (515F-806R) that include sequencer adapter sequences used in the Illumina flowcell. The microbiota signature cohort consisting of infant donor fecal samples, and gnotobiotic mouse fecal and ileal samples (n=99) was analyzed by Quantitative Insights into Microbial Ecology (QIIME) (version 1.9) [35]. Raw reads were trimmed to remove low quality bases; paired-end 3' overlapping sequences were merged using SeqPrep (https://github.com/jstjohn/SeqPrep). The open reference OTU picking protocol was used at 97% sequence identity against the Greengenes database (08/2013 release) [36]. Sequences were aligned with PyNAST [37]. Taxonomic assignments were made with the uclust consensus taxonomy assigner [38]; predicted chimeric sequences were removed using ChimeraSlayer (v20110519) (http://microbiomeutil.sourceforge.net). Data were rarefied to an even depth of 3,160 reads for the donor and colonized mouse cohort (n=99, consisting of donor fecal samples, mouse fecal samples at 2- and 3-weeks post-colonization, and mouse ileal samples), and 10,050 reads for the mouse cohort shown in Extended Data Fig. 8c (n=70, consisting of paired fecal and ileal samples from the 35 mice at 1-week post-colonization). Alpha (Shannon index) and beta diversity metrics were compared between CMA and healthy groups using Mann-Whitney-Wilcoxon test (non-parametric) and PERMANOVA with weighted UniFrac distance in R package vegan (v2.4.5) [39], respectively. Pielou's evenness index J' was computed by $J' = \frac{H'}{\ln S}$ where H' is Shannon index and S as the maximum number of OTUs. Discrete False-Discovery Rate (DS-FDR) [40] was used to

identify differentially abundant bacterial taxa between fecal communities of the CMA and healthy groups with parameters “transform_type=normdata, method=meandiff, alpha=0.10, numperm=1000, fdr_method=dsfdr” (accessed 02262018) (https://github.com/biocore/dsFDR). Compared to the Benjamini-Hochberg-FDR (BH-FDR) method, the DS-FDR method has increased power with limited sample size and is robust to sparse data structure (low proportion of non-zero values in microbe abundance table), therefore is uniquely suited for data analysis of microbe communities [40]. The DS-FDR algorithm does not compute adjusted *P*-values; instead, it estimates the false-discovery rate from a permutation test (default 1000 permutations), which controls the FDR at the desired level (0.10). As such, it computes the raw *P*-values, test statistics and rejected hypotheses in the output (Supplementary Table 3 **and** Supplementary Table 5). In each comparison, OTUs present in less than 4 samples were removed prior to applying the DS-FDR test. Linear discriminant analysis effect size (LEfSe) was used to identify genera significantly enriched in CMA or healthy groups compared to the other, using the per-sample normalization value of 1,000,000 and default values for other parameters [41]. In LEfSe analysis, linear discriminant analysis (LDA) score was computed for taxa differentially abundant between the two groups. A taxon at $P<0.05$ (Kruskal-Wallis test) and $\log10(\text{LDA}) \geq 2.0$ (or ≤ -2.0) was considered significant. For Fig. 2a, after differential abundance testing in donor CMA vs healthy comparison using DS-FDR, we further filtered the significant OTUs by requiring presence in at least two mouse groups, leaving a total of 58 OTUs for further analysis. An OTU ratio was calculated by dividing the total number of potentially protective OTUs (more abundant in healthy) by the total number of potentially non-protective OTUs (more abundant in CMA) per sample. In addition, an OTU abundance score was computed taking into consideration the abundance of 58 OTUs identified in CMA relative to healthy donor fecal samples shown in Fig. 2a. First, data transformation was applied on the relative abundance to bring the signal close to Gaussian distribution. The relative abundance of each OTU was multiplied by a constant (1×10^6) to bring all values to larger than 1, log10 transformed, and scaled by dividing the value by their root mean square across samples. The abundance of potentially non-protective OTUs was multiplied by (−1). Next, the sum of the transformed abundance of the 58 OTUs was calculated to generate the aggregate score. To validate the OTU ratio differences in the independent cohort, we re-analyzed the 16S sequencing data of fecal samples collected from the healthy and CMA infants (n=38) in ref. 5 using the same analysis protocol described above, with data rarefied to an even depth of 6,424 reads. Among the 58 OTUs shown in Fig. 2a, 55 OTUs were assigned with known reference IDs and 3 with new reference IDs (Supplementary Table 3). The new reference OTU IDs are not comparable between different analysis cohorts, hence we focused on the OTUs with known reference IDs. Out of 55 known OTUs, 52 were matched in the reanalyzed independent cohort and used for calculation of protective/non-protective OTU ratio depicted in Extended Data Fig. 6.

Food allergen sensitization and challenge.

Protocols were adapted from ref. [7]. All mice were weaned onto a plant-based mouse chow (Purina Lab Diet® 5K67) at 3 weeks of age. GF mice received autoclaved sterile water. For mice colonized with feces from infant donors, or monocolonized with *A. caccae*, the drinking water was replaced by formula four hours prior to colonization. Mice colonized

with healthy feces or *A.caccae* received Enfamil; CMA colonized mice received Nutramigen (both from Mead Johnson). On day 0, one week post weaning (GF) or colonization (healthy/*A.caccae*/CMA), all mice were fasted for 4 hours and then given a gavage of 200mM sodium bicarbonate. 30 minutes later, mice were given 20mg BLG (Sigma) plus 10μg CT (List Biologicals). This protocol was repeated weekly for 5 weeks. For formula-fed mice, formula was replaced by sterile water for the week after the last sensitization. Prior to challenge on day 42, mice were fasted for 4 hours and given sodium bicarbonate by gavage. Two doses of 100mg BLG each were then administered via intragastric gavage 30 minutes apart. Core body temperature was measured in a blinded fashion prior to allergen challenge and every 5 minutes after the first challenge until at least 30 minutes after the second challenge using a rectal probe (PhysiTemp). Serum was collected 1 hour after the second challenge to measure mMCPT-1 levels. Serum was collected 24 hours after challenge for antibody measurements.

ELISAs.

mMCPT-1 was quantified in serum collected 1 hour after the second challenge according to the manufacturer's protocol (eBioscience). BLG-specific ELISAs were performed using protocols modified from ref. [7]. Briefly, plates were coated overnight at 4°C with 100μg/mL BLG in 100mM carbonate-bicarbonate buffer (pH 9.6). Plates were blocked for 2 hours at room temperature with 3% BSA. Samples were added in 1% BSA and incubated overnight at 4°C. Assays were standardized with BLG-specific antibodies (IgE or IgG1) purified on a CNBr-Sepharose affinity column from mice immunized with BLG+alum [42]. BLG-specific antibodies were detected with goat anti-mouse IgE-UNLB (Southern Biotech) and rabbit anti-goat IgG-AP (ThermoFisher) then developed with *p*-NPP (KPL Labs) or IgG1-HRP (Southern Biotech) and developed with TMB (Sigma).

For cytokine analysis spleens were harvested 24h post challenge from *A. caccae* or CMA colonized mice sensitized with BLG+CT for 5 weeks. *S*plenocytes were stimulated at a concentration of 2×10^6 cells/ml at 37°C, 10% CO_2 with 10 mg/ml BLG (Sigma) in cDMEM (with 4% FCS (HyClone), 10mM HEPES (Gibco), 100U/ml Penicillin/Streptomycin (Gibco) and 55μM 2-mercaptoethanol (Gibco). Cytokine concentrations in 72 hr culture supernatants were determined by ELISA for IL-13 and IL-4 (both from Invitrogen).

Epithelial cell isolation.

As in sensitization experiments, mice were weaned at 3 weeks of age and placed on infant formula prior to colonization. Seven days after colonization, mice were euthanized and ileum was removed. For IEC isolation, tissues were cleaned and inverted as described in ref. [43]. IECs were collected by inflating inverted tissue in Cell Recovery Solution (Corning) every 5 minutes for 30 minutes. IEC samples were lysed in TRIZol (ThermoFisher) and RNA was extracted with PureLink RNA Mini Kit (Ambion) plus on-column DNAse treatment (PureLink DNAse Set, Ambion).

RNASeq.

RNA libraries were prepared using TruSeq Stranded Total Library Preparation Kit with Ribo-Zero human/mouse/rat (Illumina). Samples were sequenced at the University of Chicago Functional Genomics Core, using 50 bp single reads chemistry in a HiSeq2500

instrument, with sequencing replicates in two lanes. The quality of raw reads was assessed by FastQC (v0.11.5) [44]. The QC30 score across 39 RNAseq samples was 96.81%±0.06% (mean±S.E.M), which represents the percentage of bases with quality score ≥ Q30. Alignment to the mouse reference transcriptome was performed with Gencode gene annotation (vM16, GRCm38) by Kallisto (v0.43.1) with the strand-specific mode [45]. This mode implements a kmer-based pseudoalignment algorithm to accurately quantify transcripts from RNASeq data while robustly detecting errors in the reads. The average mapping rate was 62.77%±1.10% (mean±S.E.M) based on the Kallisto pseudoalignments to the reference transcriptome. On average, 35 million raw sequencing reads were generated per sample, and 22 million were mapped to transcriptome using Kallisto. Transcript-level abundance was quantified specifying strand-specific protocol, summarized into gene level using tximport (v1.4.0) [46], normalized by trimmed mean of M values (TMM) method, and log2-transformed. Genes expressed in at least 3 samples (counts per million of reads (CPM)>3) were kept for further analysis. Genes differentially expressed between groups were identified using limma voom algorithm with precision weights (v3.34.5) [47]. duplicateCorrelation function was used to estimate the correlation among mouse samples with Donor (1 to 8) as the blocking factor. lmFit function was used to fit all mouse samples (n=39, 18 CMA-colonized, 18 healthy-colonized, and 3 GF) into one linear model incorporating the correlation structure computed from above. Contrasts were set as CMA versus healthy, CMA versus GF and healthy versus GF to identify DEGs in each comparison. Genes that are significantly differentially expressed between CMA and healthy, and also different from GF mice were identified using a two-step procedure: (1) Genes were detected as different in CMA vs healthy comparison with fold change ≥1.5 or ≤−1.5 at false-discovery rate (FDR) corrected p-value smaller than 0.10; (2) Genes from step (1) were further filtered by fold change ≥1.5 or ≤−1.5 in CMA vs GF or healthy vs GF comparison at FDR 0.05. A more stringent FDR threshold (0.05) was applied in step (2) to prioritize potentially true positives when compared to the negative control (GF). Multiple testing correction was performed using Benjamini-Hochberg FDR (BH-FDR) method [48]. A total of 32 DEGs passed these thresholds, which represent four types of gene expression changes in colonized mice: (1) Up in healthy: genes that are up-regulated in healthy mice relative to both CMA and GF; (2) Up in CMA: genes that are up-regulated in CMA mice relative to both healthy and GF; (3) Down in healthy: genes that are down-regulated in healthy mice relative to both CMA and GF; and (4) Down in CMA: genes that are down-regulated in CMA mice relative to healthy and GF. The four groups of DEGs are shown in **Figs.** 3a and 4a. Gene Ontology and KEGG pathways significantly enriched in the 32 DEGs of interest were identified using clusterprofiler (v3.6.0) [49] at false-discovery rate (FDR) corrected p-value smaller than 0.10 (BH-FDR method, hypergeometric test). The DEGs were split into two groups for this analysis; (1) Healthy included all genes that were Up in healthy and Down in CMA and (2) CMA included all genes that were Up in CMA and Down in Healthy. Correlation between DEGs and ileal OTUs significantly differentially abundant between CMA and healthy samples were computed using Spearman's rank correlation method, followed by applying filters to (1) keep the OTUs that show significant correlation with at least 1 DEG from the designated group at $P<0.05$. For potentially protective OTUs (more abundant in healthy), they are correlated with genes from group "Up in healthy" or "Down in healthy"; for potentially non-protective OTUs (more abundant in CMA), they are

correlated with genes from group “Up in CMA” or “Down in CMA”; (2) keep the OTUs that show relatively consistent trend of positive correlation (Spearman’s ρ>0.20) across at least 60% of the DEGs from the designated group. For potentially protective OTUs, they are correlated with genes from group “Up in healthy” and “Down in CMA” joined; for potentially non-protective OTUs, they are correlated with genes from group “Up in CMA” and “Down in healthy” joined; (3) keep OTUs present in at least 3 CMA and 3 healthy mice. 9 ileal OTUs passed these correlation filters and are shown in Fig. 4a. Correlation between the relative abundance of OTUs and gene expression were calculated using Spearman’s correlation method with samples that are above the limit of detection for the assay.

qPCR.

Gene expression was measured by qPCR as described in ref [7]. In brief, cDNA was prepared from RNA using the iScript cDNA Synthesis kit (BioRad). Gene expression was measured with PowerUp SYBR green master mix (Applied Biosystems) according to the manufacturer’s instructions. Primers are listed in Supplementary Table 7. Expression of genes of interest was normalized to *Hprt.* Relative expression was measured using ΔΔCt centered around the geometric mean; GF mice were used as a reference.

The presence of *A. caccae* in fecal and ileal samples was confirmed using qPCR as described in ref. [24]. Bacterial DNA was extracted using the Power Soil DNA Isolation Kit (MoBio) and qPCR was performed using PowerUp SYBR green master mix (Applied Biosystems) using 4μl of each primer at 10μM working dilution and 2μl of bacterial DNA. Primers are listed in Supplementary Table 6. The cycling conditions for the reaction consisted of an activation cycle of 50°C for 2min followed by one cycle of 95°C for 10min and 40 cycles at 94°C for 20sec, 55°C for 20sec and 72°C for 50sec. The fluorescent probe was detected in the last step of this cycle. A melt curve was performed at the end of the PCR to confirm specificity of PCR product. Relative abundance is expressed as 2^{-Ct} normalized to total 16S rRNA copies per g fecal material and multiplied by a constant (1×10^{25}) to bring all values above 1.

Histopathologic analysis.

For histological analysis 3mm pieces of mid-colon and mid-ileum tissue were fixed in either 10% formalin for H&E staining or Carnoy’s fixative for Periodic-acid Schiff (PAS) staining. Sectioning and staining were performed by the Human Tissue Resource Center at the University of Chicago. All sections were reviewed by a GI pathologist in a blinded fashion.

Statistical analysis.

Prism 7.0 (GraphPad) was used to perform one-way (Fig. 4f) ANOVA with Bonferroni correction for multiple comparisons and Student’s *t*-test (Fig. 4d and Extended Data Fig. 9b), as indicated in the figure legends. DS-FDR method was used to identify significant OTUs (Fig. 2a, Fig. 4c and Extended Data Fig. 9a) comparing CMA to healthy group. BH-FDR method was used for multiple testing correction in RNA-Seq analysis (Fig. 3a) and GO enrichment analysis (Fig. 3b). Shannon Diversity and Pielou’s Evenness were compared using a non-parametric Mann-Whitney-Wilcoxon test (Extended Data Fig. 3a, b). Analysis of protective/non-protective OTU ratio in the larger, independent cohort of infants was

performed using two-sided Wilcoxon rank sum test (Extended Data Fig. 7). The biological responses of different donor colonized mice to sensitization with BLG (Fig. 1a-d, Fig. 4g, Extended Data Fig. 4a, Extended Data Fig. 5a) were explored with linear mixed-effect models[50] based on restricted maximum likelihood (REML) in R (lmerTest v3.0.1)[51]. Group (GF, healthy and CMA in Fig. 1a; *A. caccae* and CMA in Fig. 4g; healthy BFD and CMA BFD in Extended Data Fig. 4a; H_2O and Enfamil in Extended Data Fig. 5a) temperature changes across time (both linear and quadratic) were modeled as *Temperature = Group + Time*Group + Time*Time*Group* with random intercepts and slopes estimated for individual mice. Contrasts of group temperature trends were performed using *t*-tests with the Benjamini-Hochberg FDR (BH-FDR) adjustment for multiple comparisons. To control for cases where groups contained multiple donors (Fig. 1a), we updated the previous model to include mice nested within each donor as a random effect and repeated the contrasts. Since the results of the two models were concordant, we chose to report the results from the first model for consistency of methods. For Fig. 1b-d, antibody concentrations were log transformed and modeled as *log(Concentration) = Group* with donors as a random effect. Contrasts for group differences were performed using the previously mentioned methods. For Fig. 4h-l, Extended Data Fig. 4b-d, Extended Data Fig. 5b-d, antibody and cytokine concentrations were log transformed and compared using *t*-tests. The data analysis commands (including the data files and R markdown files for reproducibility) are available from the authors upon request.

Data availability

The data that support the findings of this study are available from the corresponding author upon request. The 16S rRNA and RNASeq raw FastQ sequencing files were deposited into The NCBI Sequence Read Archive (SRA) and are available under the accession numbers SRP130620 and SRP130644, respectively. Additional processed data reported in this study are available upon request.

Code availability

The open-source analysis software used in this study is publicly available and referenced as appropriate. Custom codes are available from the corresponding author upon request.

Extended Data

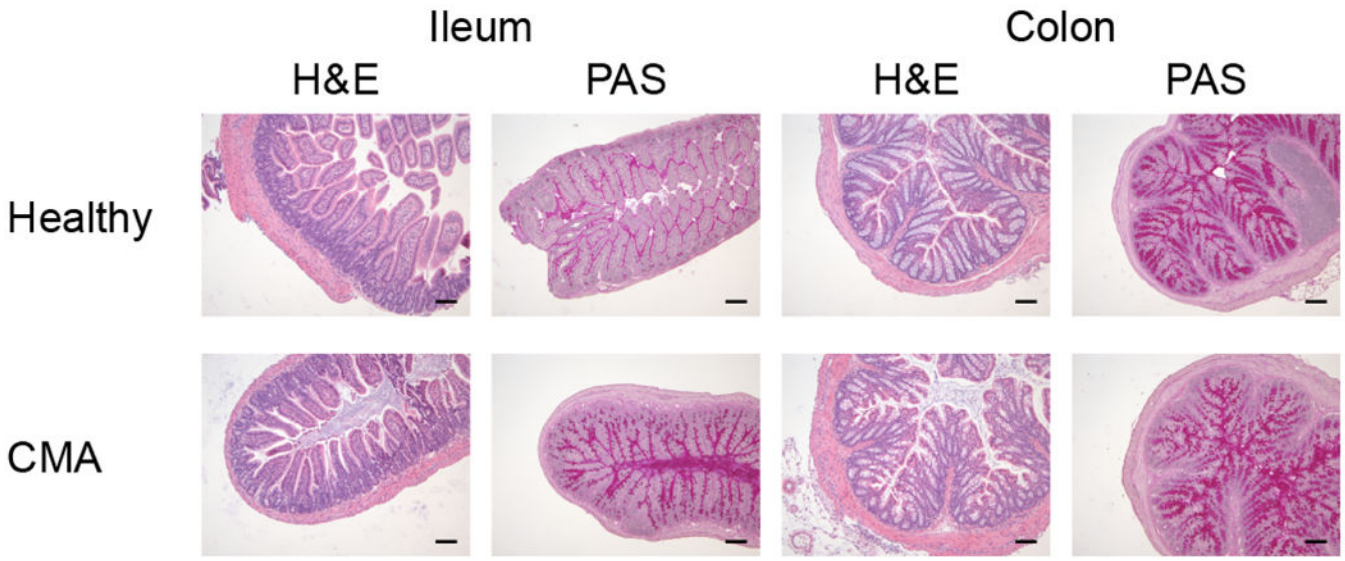

Extended Data Figure 1. Sensitization of healthy- or CMA-colonized mice with BLG+CT does not result in intestinal pathology.

Representative images of histological samples from BLG+CT sensitized healthy- or CMA-colonized mice 24 hours post-challenge for donors #1 (healthy) and #5 (CMA, see Supplementary Table 1). All sections stained with H&E or PAS, as indicated. Scale bars = 100μm.

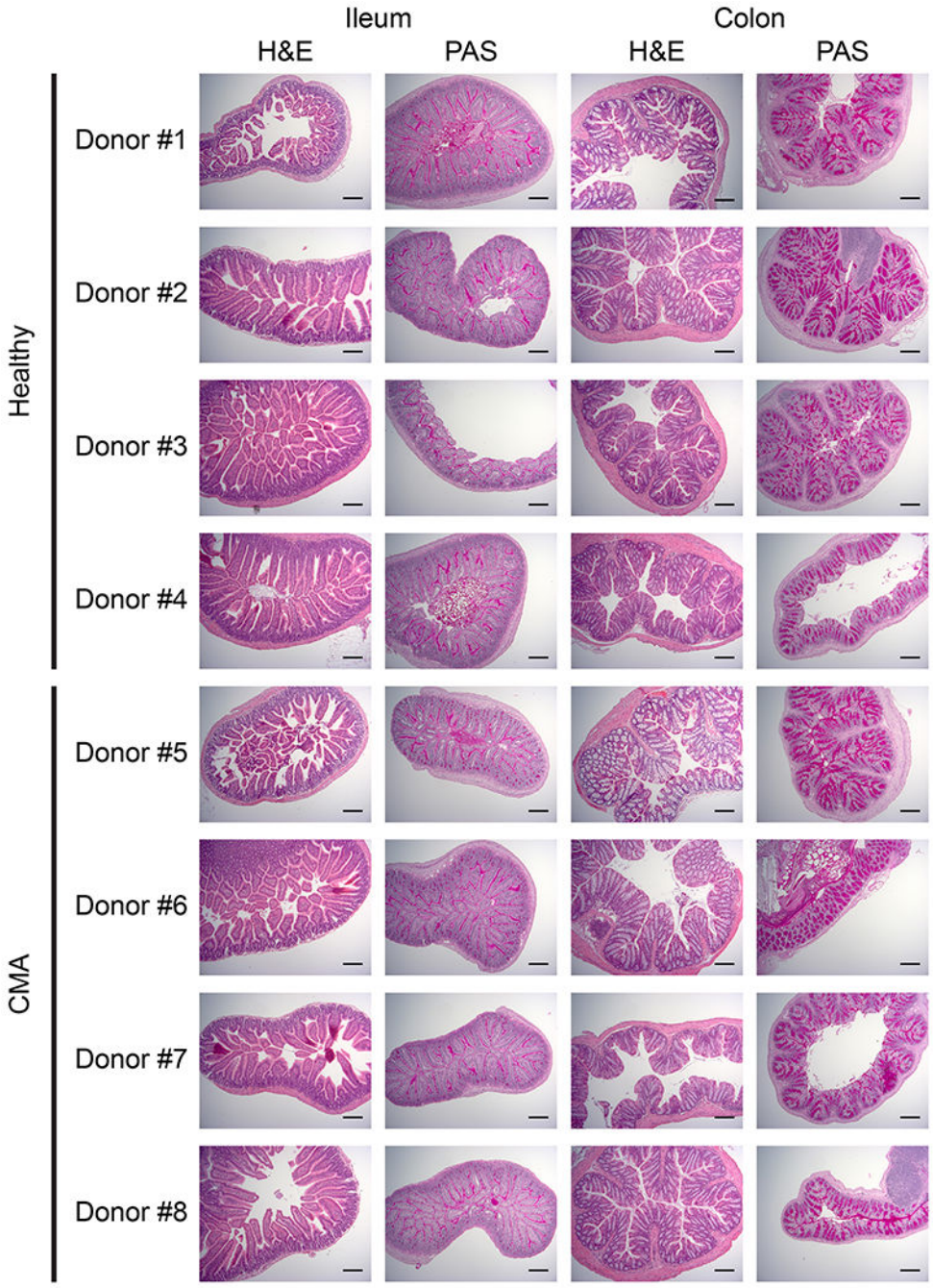

Extended Data Figure 2. Long term colonization of GF mice with feces from healthy or CMA infants does not lead to intestinal pathology.

Representative images of histological samples from unsensitized healthy- or CMA-colonized mice collected 5 to 6 months post-colonization for donors described in Supplementary Table 1. All sections stained with H&E or PAS, as indicated. Scale bars = 100μm.

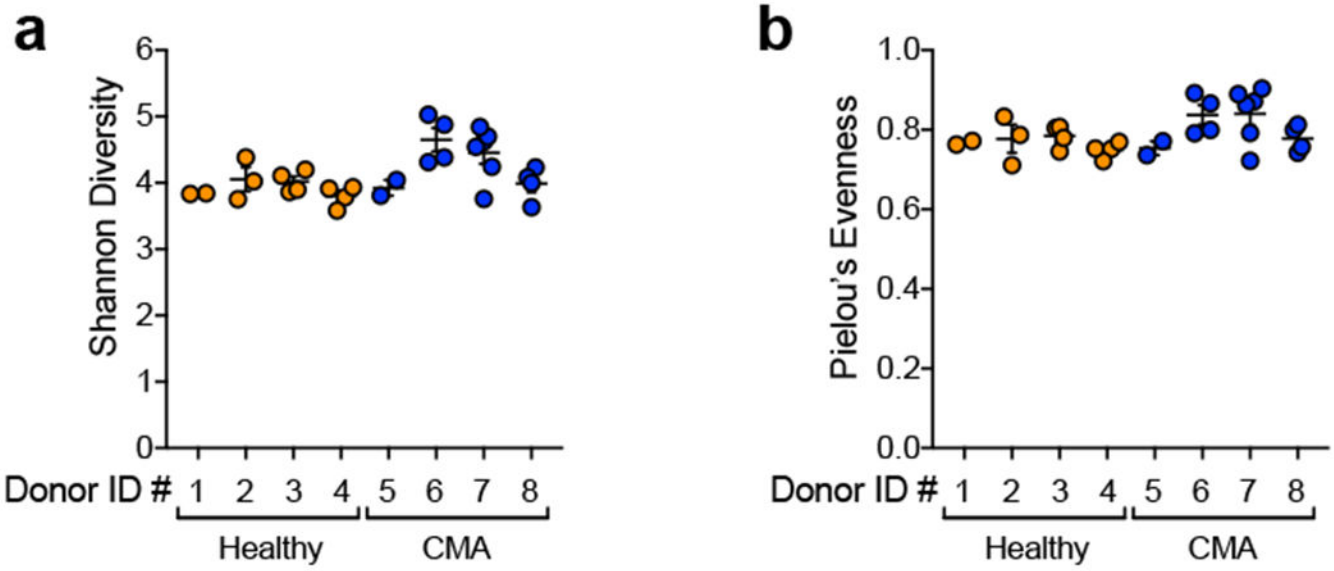

Extended Data Figure 3. Diversity analysis of fecal samples from healthy- or CMA-colonized mice.

(**a**) Shannon Diversity index and (**b**) Pielou's Evenness index in feces from healthy- (orange) and CMA- (blue) colonized mice from Fig. 2a. n=1-3 mice per colonized mouse group (8 healthy, 9 CMA) with feces taken at 2 and 3 weeks post-colonization, see Methods). Each circle represents one fecal sample, bars represent mean±S.E.M. The eight human formula-fed fecal donors are described in Supplementary Table 1.

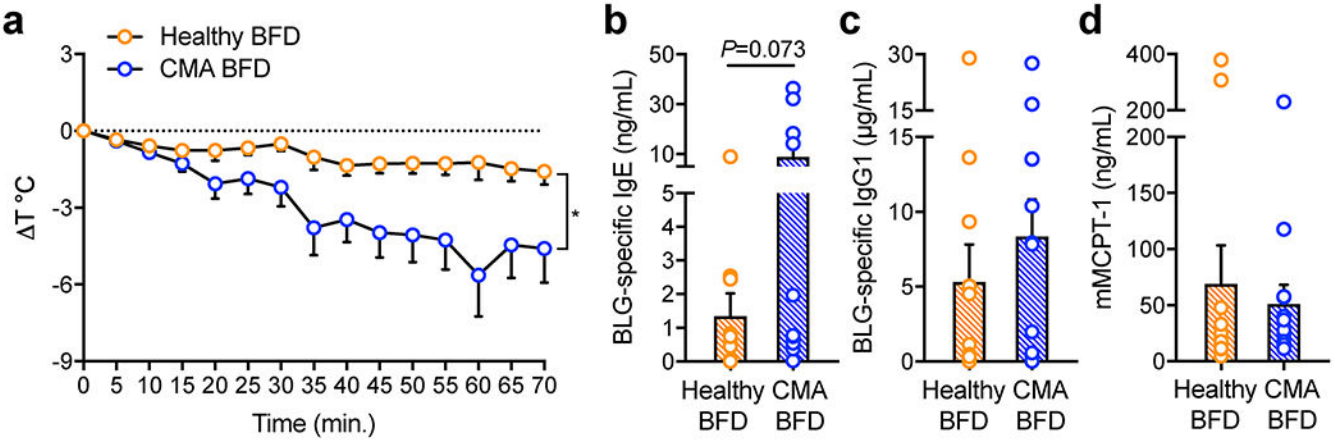

Extended Data Figure 4. Transfer of a healthy, exclusively breast-fed infant microbiota protects against an anaphylactic response to sensitization with BLG+CT.

(**a**) Change in core body temperature at indicated time points following first challenge with BLG of mice colonized with feces from breast-fed healthy or CMA donors (n=13 mice per group, pooled from at least two independent experiments). (**b**) serum BLG-specific IgE, (**c**) BLG-specific IgG1 and (**d**) mMCPT-1 from mice in **a**. Four of the BLG+CT sensitized CMA-colonized mice died of anaphylaxis following challenge. For **a**, symbols represent mean, bars represent S.E.M. For **b-d**, symbols represent individual mice, bars represent mean+S.E.M. Linear mixed-effect models were used to compare groups in **a**, two-sided

Student's *t*-test in **b** after log transformation. The two human breast-fed fecal donors are described in Supplementary Table 2. **P*<0.05.

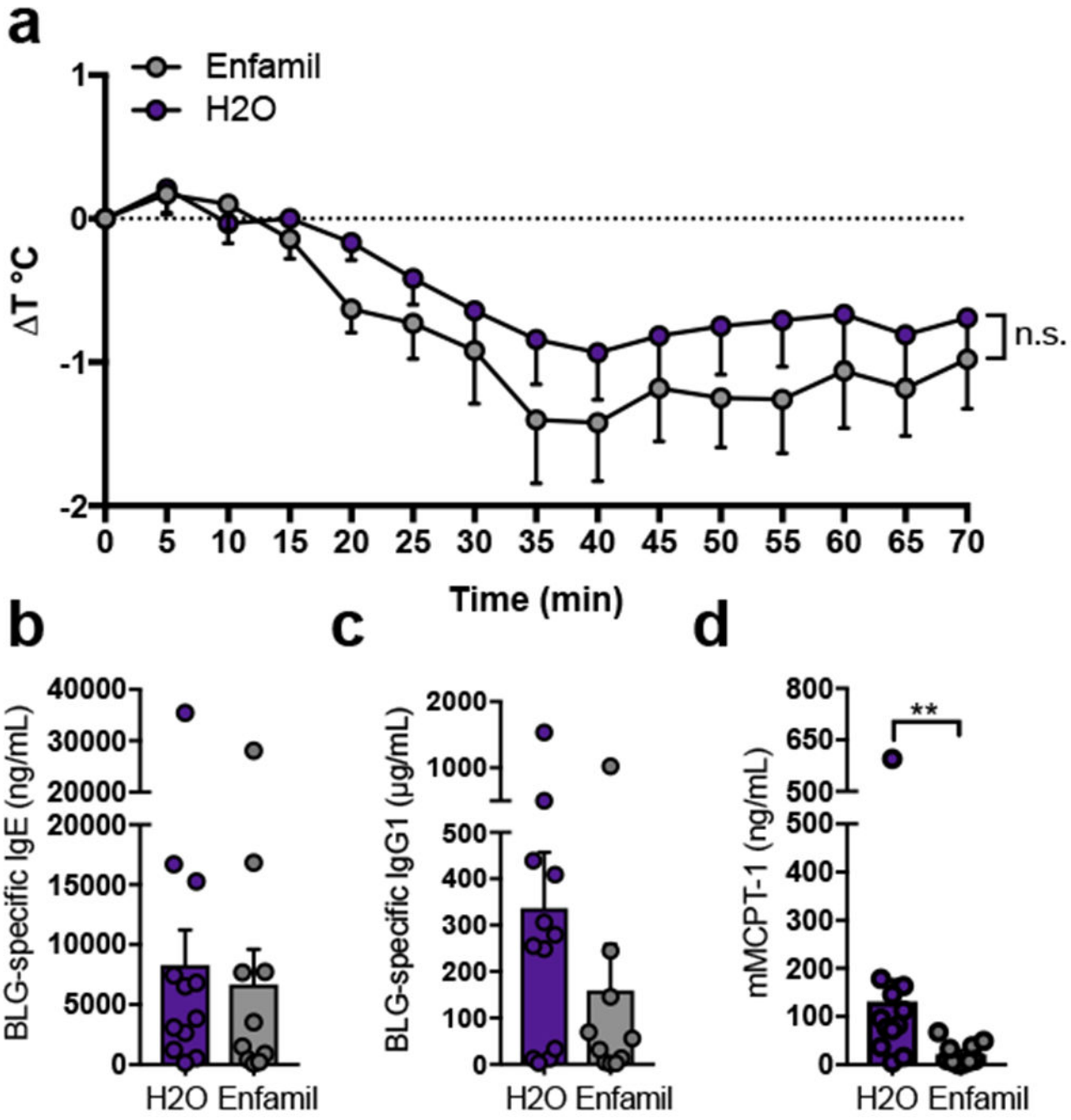

Extended Data Figure 5. Continuous exposure to cow's milk does not induce tolerance to BLG in GF mice.

GF mice fed water or Enfamil were sensitized to BLG as described in the legend to Fig. 1. (**a**) Change in core body temperature at indicated time points following first challenge with BLG of mice fed with water (n=12) or Enfamil (n=10) pooled from three independent experiments. (**b**) Serum BLG-specific IgE, (**c**) BLG-specific IgG1 and (**d**) mMCPT-1 from

mice in **a**. For **a**, circles represent mean, error bars represent S.E.M. For **b-d**, circles represent individual mice, bars represent mean+S.E.M. Linear mixed-effect models were used to compare groups in **a** and two-sided Student's *t*-test in **b-d** after log transformation. ** $P<0.01$.

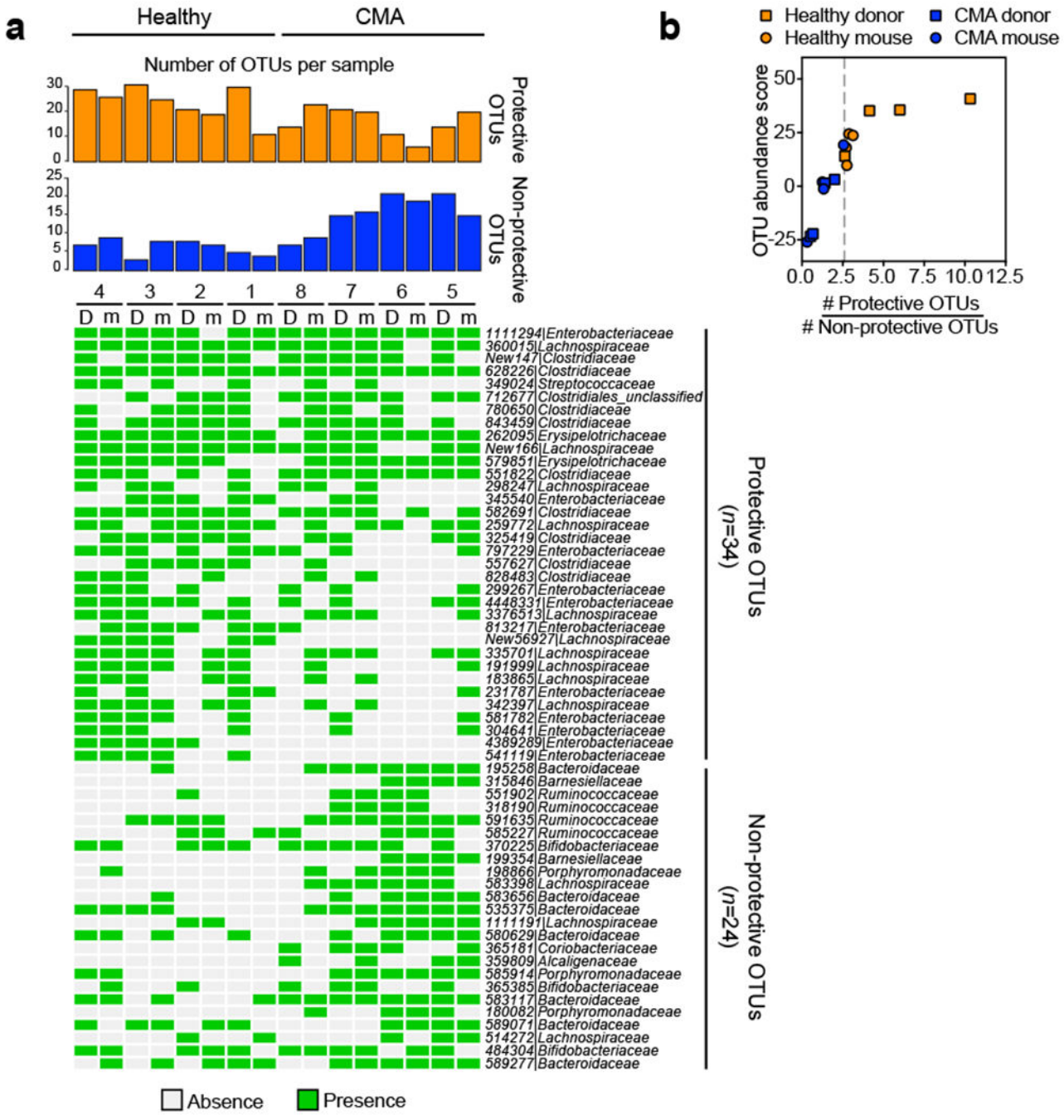

Extended Data Figure 6. Binary representation of protective and non-protective OTUs in CMA and healthy donors and colonized mouse groups

(**a**) Binary map of the presence/absence ratio of protective/non-protective OTUs in CMA and healthy donors with the same layout as Fig. 2a. Columns depict each donor (D) (n=4 in

healthy donor group, n=4 in CMA donor group, with 2 or 3 technical replicates per donor) or colonized mouse group (m) (n=8 mice in healthy group, with 1, 2, 3, 2 mice per colonized mouse group of donor #1 to #4; n=9 mice in CMA group, with 1, 2, 4, 2 mice per colonized mouse group of donor #5 to #8; for each individual mouse, 1-2 fecal samples were collected at 2 and 3 weeks post-colonization, see Methods). Rows show 58 OTUs FDR controlled at 0.10 (see Methods) in human CMA vs healthy donor comparison, present in at least 4 human fecal samples and at least two groups of colonized mice (see Supplementary Table 3). Columns depict each donor (D) or colonized mouse group (m). The bar graphs above the grid map represent the total number of potentially protective (more abundant in healthy donors; orange) and potentially non-protective (more abundant in CMA donors; blue) OTUs in each individual donor or mouse group. The grid map represents presence (green) or absence (white) of protective and non-protective OTUs in each sample. (**b**) A protective/non-protective OTU ratio was computed per individual donor or mouse group from **a**, taking into consideration the presence or absence of 58 OTUs. The donors and their murine transfer recipients are shown in squares and circles, respectively. Vertical dashed line represents a ratio of 2.6.

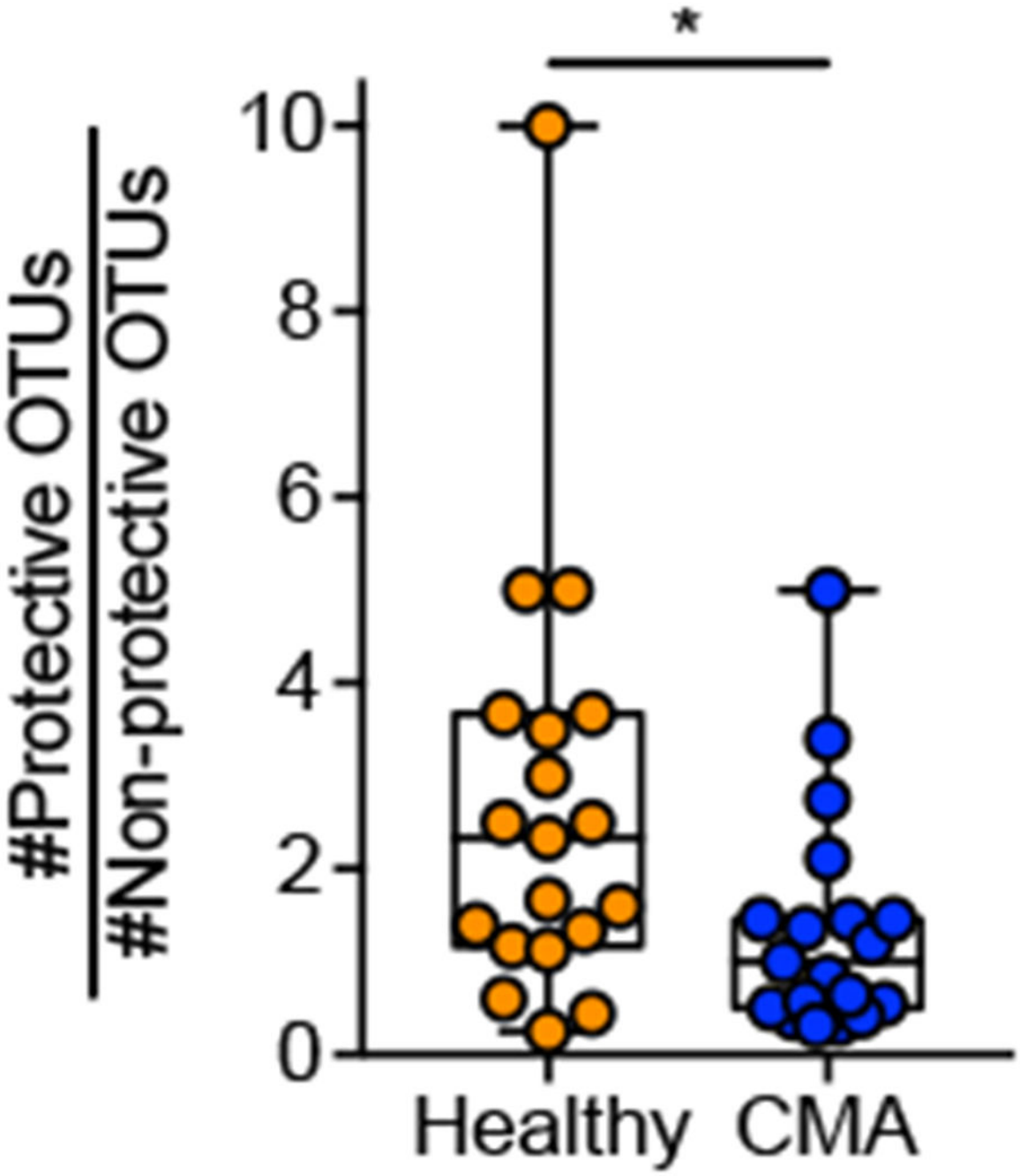

Extended Data Figure 7. Validation of protective/non-protective OTU ratio using a larger, independent cohort of healthy and CMA infant donors.

Box plots showing the protective/non-protective OTU ratio (see Fig. 2 and Extended Data Fig. 6) in fecal samples from healthy (n=19) and CMA (n=19) infants from ref. 5. The horizontal center line indicates the median, the boxes represent the 25th and 75th percentiles, and the whiskers extend to the farthest data point within a maximum of 1.5 times the interquartile range (IQR), All individual points are shown, with each circle denoting a subject. Out of the 58 OTUs shown in Fig. 2a, 55 OTUs were assigned with known reference IDs and 3 with new reference IDs. The new reference OTU IDs are not

comparable across the different analysis cohorts, therefore we focused on the OTUs with known reference IDs. Among the 55 known OTUs, 52 (29 protective OTUs and 23 non-protective OTUs) were detected in this cohort and used for the ratio calculation (see Methods). The other 3 were not detected.. Two-sided Wilcoxon rank sum test *P* value is shown. **P*<0.05.

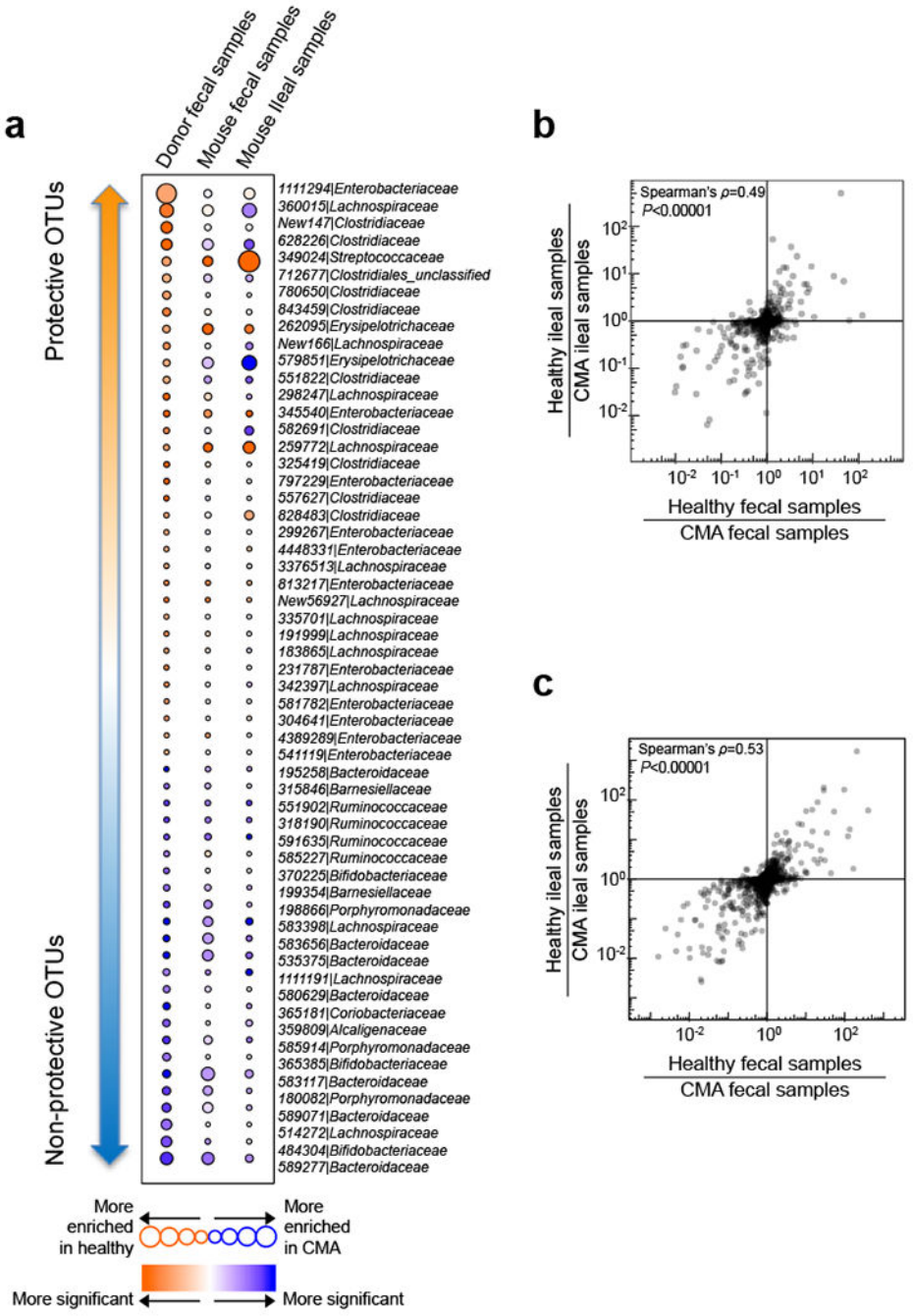

Extended Data Figure 8. The healthy vs CMA OTU abundance ratio is significantly correlated between mouse fecal and ileal samples.

(a) Bubble plots show a similar pattern in fecal (n=8 mice in healthy group, n=9 mice in CMA group, with fecal samples collected at 2 and 3 weeks post-colonization, same as in Fig. 2a) and ileal samples (n=22 mice in healthy group, n=25 mice in CMA group) from healthy- and CMA-colonized mice. 58 OTUs significantly differentially abundant between CMA and healthy donors are shown in the same order as in Fig. 2a. The size of the circle indicates the magnitude of relative abundance enrichment towards either CMA or healthy. Color intensity indicates the statistical significance computed using the DS-FDR permutation test (see Methods). (b and c) The healthy vs CMA OTU abundance ratio is significantly correlated between mouse fecal and ileal samples. Each dot represents one individual OTU. For b, for each OTU, its average abundance was calculated at the group level among 8 healthy-colonized and 9 CMA-colonized mice for the fecal samples, and among 22 healthy-colonized and 25 CMA colonized mice for the ileal samples. The ratios of OTU abundance in the feces are plotted on the x-axis with the ratio of OTU abundance in the ileum on the y-axis. For c, n=35 (15 healthy-colonized and 20 CMA-colonized) mice pooled from at least two independent experiments were used for the calculation of both the fecal and ileal OTU abundance ratio, where fecal and ileal samples were collected from the same individual mice. For further detail see Methods.

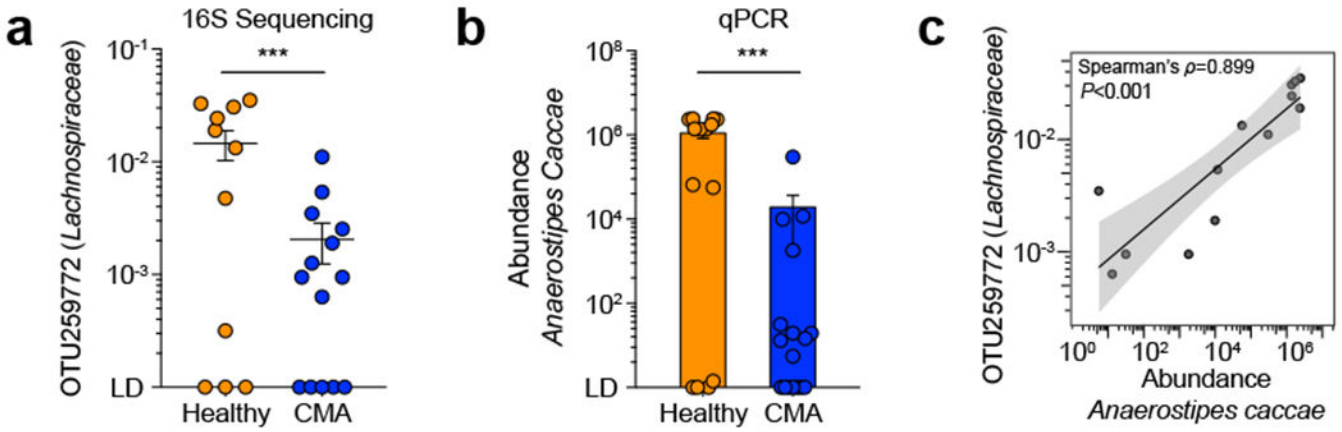

Extended Data Fig. 9. Abundance of OTU259772 (*Lachnospiraceae*) and *Anaerostipes caccae* are correlated in fecal samples from healthy- and CMA-colonized mice.

(**a**) Abundance of OTU259772 (*Lachnospiraceae*) from the 16S data set and (**b**) abundance of *Anaerostipes caccae* by qPCR in fecal samples from healthy-colonized (n=7) and CMA-colonized (n=8) mice from Fig. 2. For each individual mouse, 1-2 fecal samples were collected at 2 and 3 weeks post-colonization. LD indicates samples that were below the limit of detection for the assay. (**c**) Spearman's correlation between abundance of OTU259772 (*Lachnospiraceae*) (16S sequencing) and abundance of *Anaerostipes caccae* (qPCR) in fecal samples from healthy- and CMA-colonized mice from Fig. 2. Fecal samples that were above LD in both 16S and qPCR experiments are shown (n=13). Each circle represents one fecal sample. For **a** and **b**, bars show mean+S.E.M. For **c**, shaded bands indicate 95% confidence interval fitted by linear regression. DS-FDR method was used to compare groups in **a**, two-sided Student's *t*-test in **b**. ***$P<0.001$.

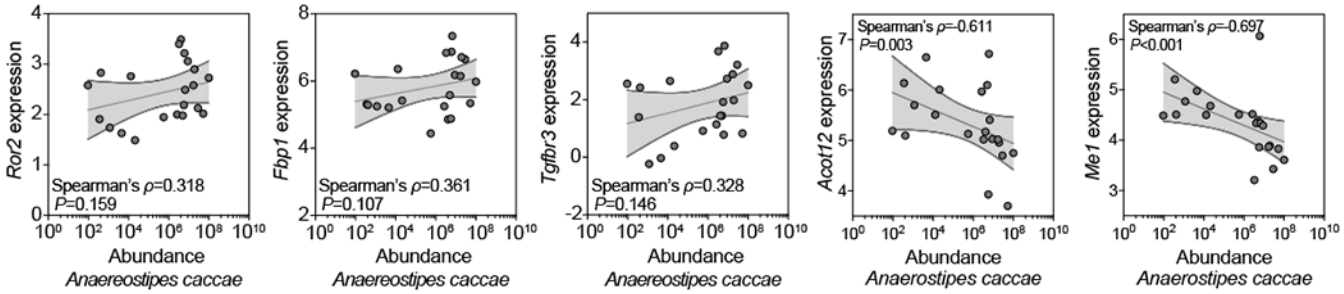

Extended Data Figure 10.

Spearman's correlation between abundance of *Anaerostipes caccae* by qPCR and RNA-Seq expression of *Ror2, Fbp1, Tgfbr3, Acot12* and *Me1* in ileal IECs (see Fig. 3a). Circles show individual mice and shaded bands indicate 95% confidence interval fitted by linear regression. n=36 (18 healthy and 18 CMA-colonized) mice pooled from at least two independent experiments. Samples with values above the limit of detection are shown (*A. caccae* abundance >0).

Supplementary Material

Refer to Web version on PubMed Central for supplementary material.

Acknowledgments

We thank the children and families for their participation in this study. We are grateful to D. Wesemann, E. Forbes-Blom, G. Nunez, M. Rothenberg, M. Alegre and J. Colson for discussion. We thank S. Wang, M. Bauer and A. Kemter for assistance with some experiments, M. Jarsulic for technical assistance of computing infrastructure, K. Hernandez for discussion of the statistical results and C. Weber for histopathological evaluation of all intestinal sections. Statistical consultation was also provided by M. Giurcanu of the UChicago Biostatistics Laboratory. We are grateful to Dr. B. Theriault and her staff at the University of Chicago Gnotobiotic Research Animal Facility for superb animal care and experimental support. This work was supported by the Sunshine Foundation (CRN), a pilot award from the UChicago Institute for Translational Medicine (CTSA ULI TR000430, CRN), National Institutes of Health Grant AI106302 (CRN), NIDDK P30DK42086 (DAA) and the Italian Ministry of Health (Grant PE-2011-02348447, RBC). The Center for Research Informatics is funded by the Biological Sciences Division at the University of Chicago with additional support provided by The Institute for Translational Medicine/Clinical and Translational Award (NIH 5UL1TR002389-02), and The University of Chicago Comprehensive Cancer Center Support Grant (NIH P30CA014599). Bioinformatics analysis was performed on Gardner High-Performance Computing clusters at the Center for Research Informatics at the University of Chicago. A provisional US patent application (62/755,945) was filed on 11/5/18.

References

1. Sicherer SH, et al. Critical Issues in Food Allergy: A National Academies Consensus Report. Pediatrics (2017).
2. Iweala OI & Burks AW Food Allergy: Our Evolving Understanding of Its Pathogenesis, Prevention, and Treatment. Curr Allergy Asthma Rep 16, 37 (2016). [PubMed: 27041704]
3. Wesemann DR & Nagler CR The Microbiome, Timing, and Barrier Function in the Context of Allergic Disease. Immunity 44, 728–738 (2016). [PubMed: 27096316]
4. Plunkett CH & Nagler CR The Influence of the Microbiome on Allergic Sensitization to Food. J Immunol 198, 581–589 (2017). [PubMed: 28069753]
5. Berni Canani R, et al. Lactobacillus rhamnosus GG-supplemented formula expands butyrate-producing bacterial strains in food allergic infants. Isme j 10, 742–750 (2016). [PubMed: 26394008]
6. Bunyavanich S, et al. Early-life gut microbiome composition and milk allergy resolution. J Allergy Clin Immunol 138, 1122–1130 (2016). [PubMed: 27292825]

7. Stefka AT, et al. Commensal bacteria protect against food allergen sensitization. Proc Natl Acad Sci U S A 111, 13145–13150 (2014). [PubMed: 25157157]
8. Dominguez-Bello MG, et al. Delivery mode shapes the acquisition and structure of the initial microbiota across multiple body habitats in newborns. Proc Natl Acad Sci U S A 107, 11971–11975 (2010). [PubMed: 20566857]
9. Mueller NT, Bakacs E, Combellick J, Grigoryan Z & Dominguez-Bello MG The infant microbiome development: mom matters. Trends Mol Med 21, 109–117 (2015). [PubMed: 25578246]
10. Blanton LV, et al. Gut bacteria that prevent growth impairments transmitted by microbiota from malnourished children. Science 351(2016).
11. Cahenzli J, Koller Y, Wyss M, Geuking MB & McCoy KD Intestinal microbial diversity during early-life colonization shapes long-term IgE levels. Cell Host Microbe 14, 559–570 (2013). [PubMed: 24237701]
12. Pabst O & Mowat AM Oral tolerance to food protein. Mucosal Immunol 5, 232–239 (2012). [PubMed: 22318493]
13. Honda K & Littman DR The microbiota in adaptive immune homeostasis and disease. Nature 535, 75–84 (2016). [PubMed: 27383982]
14. Thaiss CA, Zmora N, Levy M & Elinav E The microbiome and innate immunity. Nature 535, 65–74 (2016). [PubMed: 27383981]
15. Yanez AJ, et al. Broad expression of fructose-1,6-bisphosphatase and phosphoenolpyruvate carboxykinase provide evidence for gluconeogenesis in human tissues other than liver and kidney. J Cell Physiol 197, 189–197 (2003). [PubMed: 14502558]
16. Ostroukhova M, et al. The role of low-level lactate production in airway inflammation in asthma. Am J Physiol Lung Cell Mol Physiol 302, L300–307 (2012). [PubMed: 22080752]
17. Zhu Y, et al. NPM1 activates metabolic changes by inhibiting FBP1 while promoting the tumorigenicity of pancreatic cancer cells. Oncotarget 6, 21443–21451 (2015). [PubMed: 26068981]
18. Berger CN, et al. Citrobacter rodentium Subverts ATP Flux and Cholesterol Homeostasis in Intestinal Epithelial Cells In Vivo. Cell Metab (2017).
19. Zhang M, Zola H, Read L & Penttila I Identification of soluble transforming growth factor-beta receptor III (sTbetaIII) in rat milk. Immunol Cell Biol 79, 291–297 (2001). [PubMed: 11380683]
20. Miyoshi H, Ajima R, Luo CT, Yamaguchi TP & Stappenbeck TS Wnt5a potentiates TGF-beta signaling to promote colonic crypt regeneration after tissue injury. Science 338, 108–113 (2012). [PubMed: 22956684]
21. Planer JD, et al. Development of the gut microbiota and mucosal IgA responses in twins and gnotobiotic mice. Nature 534, 263–266 (2016). [PubMed: 27279225]
22. Schwiertz A, et al. Anaerostipes caccae gen. nov., sp. nov., a new saccharolytic, acetate-utilising, butyrate-producing bacterium from human faeces. Systematic and applied microbiology 25, 46–51 (2002). [PubMed: 12086188]
23. Duncan SH, Louis P & Flint HJ Lactate-utilizing bacteria, isolated from human feces, that produce butyrate as a major fermentation product. Appl Environ Microbiol 70, 5810–5817 (2004). [PubMed: 15466518]
24. Kurakawa T, et al. Diversity of Intestinal Clostridium coccoides Group in the Japanese Population, as Demonstrated by Reverse Transcription-Quantitative PCR. PLoS One 10, e0126226 (2015). [PubMed: 26000453]
25. Donohoe DR, et al. The microbiome and butyrate regulate energy metabolism and autophagy in the mammalian colon. Cell Metab 13, 517–526 (2011). [PubMed: 21531334]
26. Byndloss MX, et al. Microbiota-activated PPAR-gamma signaling inhibits dysbiotic Enterobacteriaceae expansion. Science 357, 570–575 (2017). [PubMed: 28798125]
27. Donohoe DR, Wali A, Brylawski BP & Bultman SJ Microbial regulation of glucose metabolism and cell-cycle progression in mammalian colonocytes. PLoS One 7, e46589 (2012). [PubMed: 23029553]
28. Atarashi K, et al. Induction of colonic regulatory T cells by indigenous Clostridium species. Science 331, 337–341 (2011). [PubMed: 21205640]

29. Atarashi K, et al. Treg induction by a rationally selected mixture of Clostridia strains from the human microbiota. Nature 500, 232–236 (2013). [PubMed: 23842501]
30. Furusawa Y, et al. Commensal microbe-derived butyrate induces differentiation of colonic regulatory T cells. Nature 504, 446–450 (2013). [PubMed: 24226770]
31. Yano JM, et al. Indigenous bacteria from the gut microbiota regulate host serotonin biosynthesis. Cell 161, 264–276 (2015). [PubMed: 25860609]
32. Kim YG, et al. Neonatal acquisition of Clostridia species protects against colonization by bacterial pathogens. Science 356, 315–319 (2017). [PubMed: 28428425]
33. Noval Rivas M, et al. A microbiota signature associated with experimental food allergy promotes allergic sensitization and anaphylaxis. J Allergy Clin Immunol 131, 201–212 (2013). [PubMed: 23201093]
34. Caporaso JG, et al. Ultra-high-throughput microbial community analysis on the Illumina HiSeq and MiSeq platforms. ISME J 6, 1621–1624 (2012). [PubMed: 22402401]
35. Caporaso JG, et al. QIIME allows analysis of high-throughput community sequencing data. Nat Methods 7, 335–336 (2010). [PubMed: 20383131]
36. DeSantis TZ, et al. Greengenes, a chimera-checked 16S rRNA gene database and workbench compatible with ARB. Appl Environ Microbiol 72, 5069–5072 (2006). [PubMed: 16820507]
37. Caporaso JG, et al. PyNAST: a flexible tool for aligning sequences to a template alignment. Bioinformatics 26, 266–267 (2010). [PubMed: 19914921]
38. Edgar RC Search and clustering orders of magnitude faster than BLAST. Bioinformatics 26, 2460–2461 (2010). [PubMed: 20709691]
39. Oksanen J, et al. vegan: Community Ecology Package. R package version 2.4.5. (2017).
40. Jiang L, et al. Discrete False-Discovery Rate Improves Identification of Differentially Abundant Microbes. mSystems 2(2017).
41. Segata N, et al. Metagenomic biomarker discovery and explanation. Genome biology 12, R60 (2011). [PubMed: 21702898]
42. Bashir ME, Louie S, Shi HN & Nagler-Anderson C Toll-like receptor 4 signaling by intestinal microbes influences susceptibility to food allergy. J Immunol 172, 6978–6987 (2004). [PubMed: 15153518]
43. Nik AM & Carlsson P Separation of intact intestinal epithelium from mesenchyme. Biotechniques 55, 42–44 (2013). [PubMed: 23834385]
44. Andrew S FastQC: A quality control application for high throughput sequence data. Babraham Institute Project page: http://wwwbioinformaticsbabrahamacuk/projects/fastqc (2016).
45. Bray NL, Pimentel H, Melsted P & Pachter L Near-optimal probabilistic RNA-seq quantification. Nat Biotechnol 34, 525–527 (2016). [PubMed: 27043002]
46. Soneson C, Love MI & Robinson MD Differential analyses for RNA-seq: transcript-level estimates improve gene-level inferences. F1000Res 4, 1521 (2015). [PubMed: 26925227]
47. Law CW, Chen Y, Shi W & Smyth GK voom: Precision weights unlock linear model analysis tools for RNA-seq read counts. Genome biology 15, R29 (2014). [PubMed: 24485249]
48. Benjamini Y & Hochberg Y Controlling the False Discovery Rate: a Practical and Powerful Approach to Multiple Testing. J.R. Statist. Soc. B 57, 289–300 (1995).
49. Yu G, Wang LG, Han Y & He QY clusterProfiler: an R package for comparing biological themes among gene clusters. OMICS 16, 284–287 (2012). [PubMed: 22455463]
50. Pinheiro JC & Bates DM Mixed-Effects in Models S and S-Plus, (Springer, New York, 2000).
51. Kuznetsova A, Brockhoff PB, Rune H & Christensen B lmerTest Package: Tests in Linear Mixed Effects Models. Journal of Statistical Software 82, 1–26 (2017).
52. Lenth R emmeans: Estimated Marginal Means, aka Least-Squares Means.R package version 1.2.3. https://CRAN.R-project.org/package=emmeans (2018).
53. Satterthwaite FE Synthesis of variance. Psychometrika 6, 309–316 (1941).
54. Upadhyay V, et al. Lymphotoxin regulates commensal responses to enable diet-induced obesity. Nat Immunol 13, 947–953 (2012). [PubMed: 22922363]
55. Liu X, et al. Warburg effect revisited: an epigenetic link between glycolysis and gastric carcinogenesis. Oncogene 29, 442–450 (2010). [PubMed: 19881551]

56. Roelen BA, Lin HY, Knezevic V, Freund E & Mummery CL Expression of TGF-beta s and their receptors during implantation and organogenesis of the mouse embryo. Dev Biol 166, 716–728 (1994). [PubMed: 7813789]

57. Ellis JM, Bowman CE & Wolfgang MJ Metabolic and tissue-specific regulation of acyl-CoA metabolism. PLoS One 10, e0116587 (2015). [PubMed: 25760036]

58. Al-Dwairi A, Pabona JM, Simmen RC & Simmen FA Cytosolic malic enzyme 1 (ME1) mediates high fat diet-induced adiposity, endocrine profile, and gastrointestinal tract proliferation-associated biomarkers in male mice. PLoS One 7, e46716 (2012). [PubMed: 23056418]

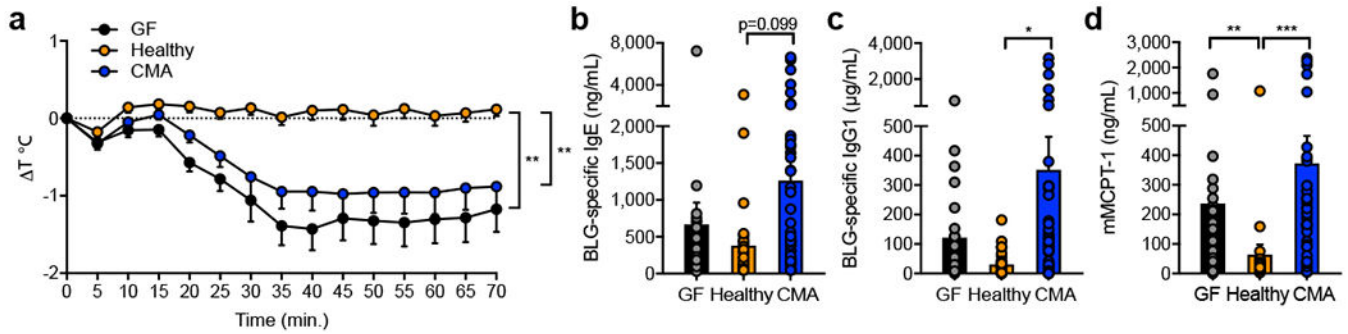

Figure 1. Transfer of healthy, but not CMA, infants' microbiota protects against an allergic response to food.

(**a**) Change in core body temperature at indicated time points following first challenge with BLG in BLG + CT sensitized GF mice and in mice colonized with feces from each of 8 donors (4 healthy, 4 CMA, see Supplementary Table 1) n=42 (CMA), 31 (healthy) and 24 (GF) mice with 9-12 mice for each of the 8 donors, pooled from two independent experiments (**b**) Serum BLG-specific IgE, (**c**) BLG-specific IgG1 and (**d**) mMCPT-1 from mice in **a**. For **a**, circles represent mean, error bars represent S.E.M. For **b-d**, circles represent individual mice, bars represent mean+S.E.M. Linear mixed-effect models were used to compare groups in **a-d** with Benjamini-Hochberg FDR (BH-FDR) method for multiple testing correction. **P*<0.05, ***P*<0.01 ****P*<0.001.

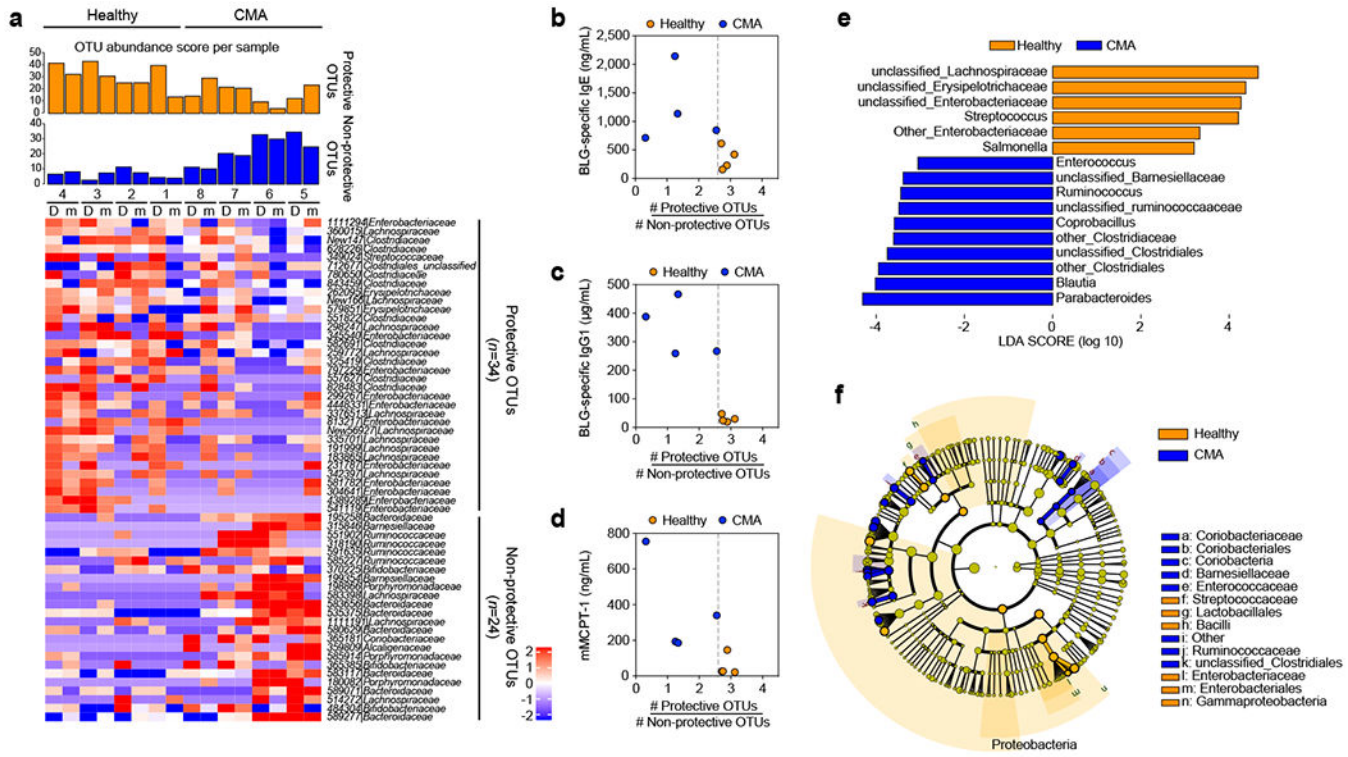

Figure 2. Analysis of fecal samples from eight human infant donors reveals taxonomic signatures that correlate with allergic phenotype.

(**a**) Heatmap of OTUs differentially abundant between CMA and healthy donors. Rows show 58 OTUs identified as different at false-discovery rate (FDR) controlled at 0.10 and present in at least 4 human fecal samples and at least two groups of colonized mice (see Supplementary Table 3). Columns depict each donor (D). For **a,** *n*=2-3 technical replicates per donor, *n*=1-3 mice per colonized mouse group with feces taken at 2 and 3 weeks post-colonization (see Methods). The bar graphs above the heatmap represent the abundance score of potentially protective (orange) or non-protective (blue) OTUs calculated for each donor or mouse group. (**b-d**) The ratio of protective over non-protective OTUs (see Extended Data Fig. 6b) derived from colonized mice in **a** plotted against levels of (**b**) BLG-specific IgE, (**c**) BLG-specific IgG1, and (**d**) mMCPT-1 from all mice in Figure 1. Each circle represents average results from all mice colonized with each of the four healthy (orange) or CMA (blue) donor's feces. (**e**) LEfSe analysis of genera that are significantly enriched in healthy-colonized mice (orange) or CMA-colonized mice (blue) from samples in **a** (n=8 mice in healthy group, n=9 mice in CMA group, with fecal samples collected at 2 and 3 weeks post-colonization). (**f**) Cladogram showing the community composition of colonized mouse samples from **a**, with the taxa detected as differentially abundant by LEfSe analysis colored by group (healthy=orange, CMA=blue). The discrete FDR (DS-FDR) method was used to compare groups in **a** and Kruskal-Wallis test in **e** (see Methods).

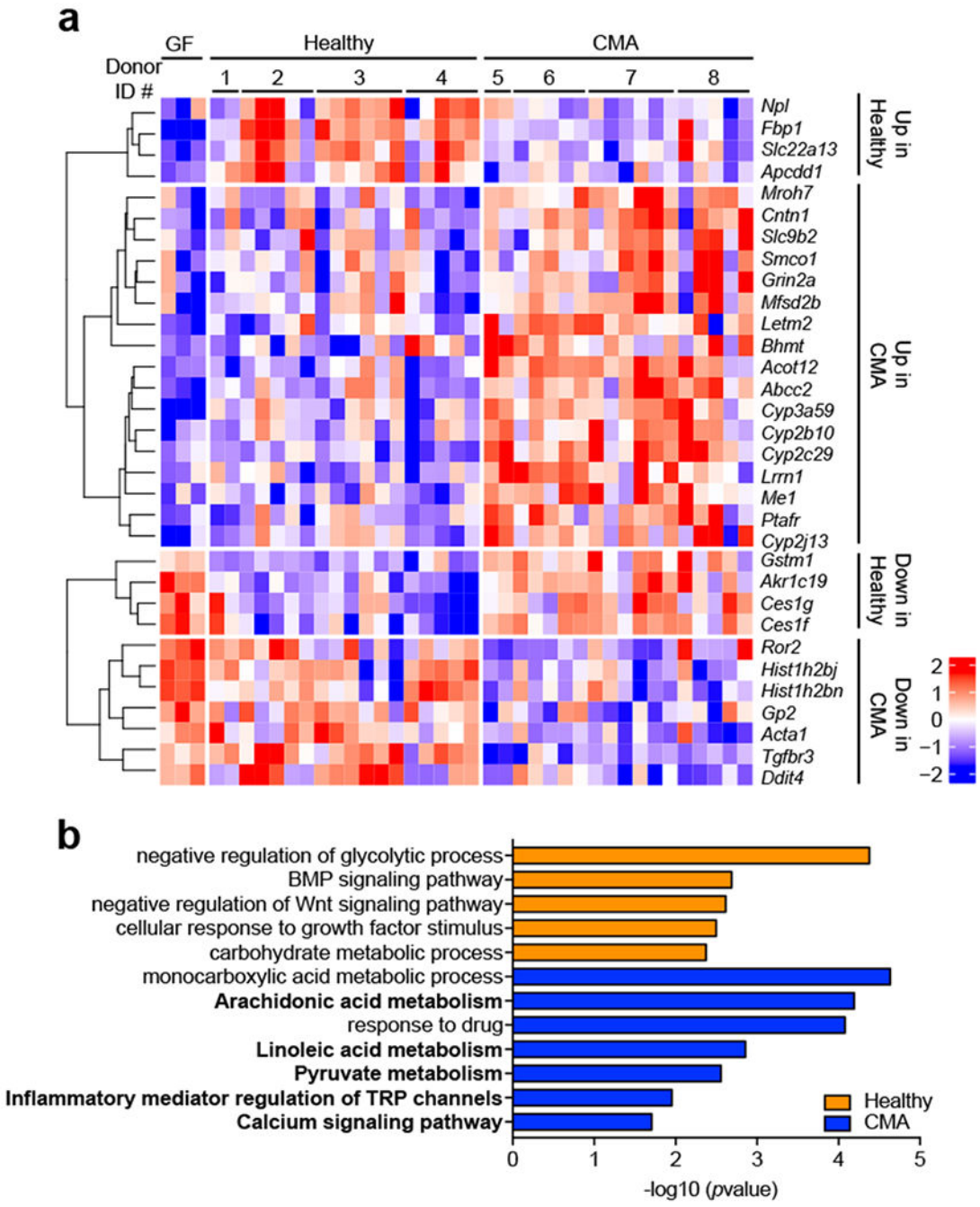

Figure 3. Unique ileal transcriptome signatures distinguish healthy- and CMA-colonized mice.

(**a**) Heatmap of 32 differentially expressed genes (DEGs) in ileal IECs isolated from GF (n=3), healthy-colonized (n=18) or CMA-colonized (n=18) mice pooled from at least two independent experiments at seven days post-colonization (see Supplementary Table 4). Each column depicts an individual mouse colonized with donor feces as indicated. Four types of gene expression changes are shown: (1) Up in healthy: genes that are up-regulated in healthy mice relative to both CMA and GF; (2) Up in CMA: genes that are up-regulated in CMA mice relative to both healthy and GF; (3) Down in healthy: genes that are down-regulated in

healthy mice relative to both CMA and GF; and (4) Down in CMA: genes that are down-regulated in CMA mice relative to healthy and GF. (**b**) Gene Ontology (GO) terms and KEGG pathways (bold) significantly enriched in DEGs from **a** that are associated with healthy- (orange) or CMA- (blue) colonized mice. Hypergeometric test was used in **b** with the Benjamini-Hochberg FDR (BH-FDR) method for multiple testing correction (see Methods).

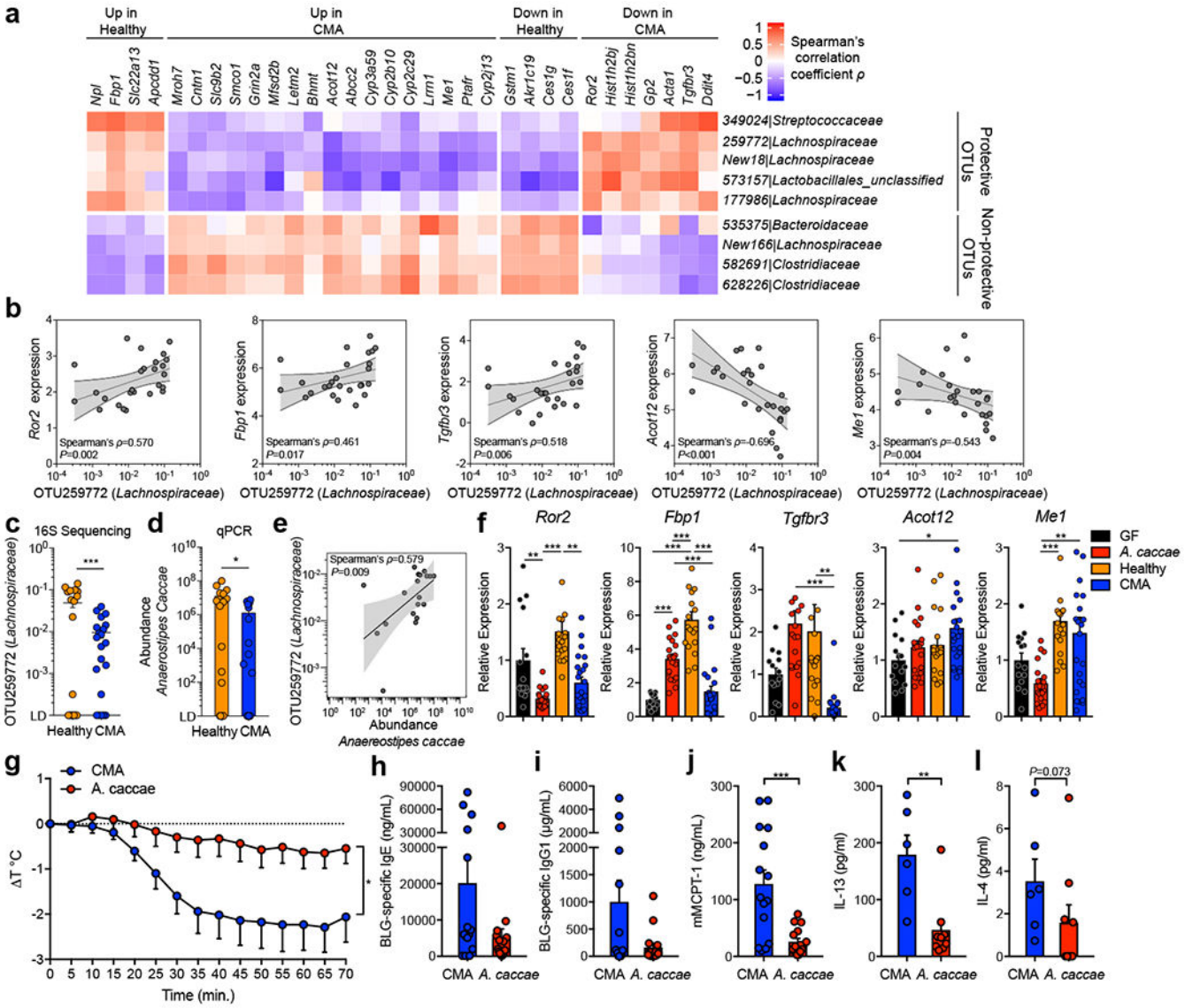

Figure 4. Correlation of ileal OTUs with DEGs in the ileum of healthy-colonized mice identifies a Clostridial species, *A. caccae*, that protects against an allergic response to food.

(**a**) Heatmap showing Spearman's rank correlation coefficient between relative abundance of ileal OTUs (row) and expression of DEGs (column) from CMA vs healthy mouse ileal IEC samples (see Fig. 3a and Methods). (**b**) Spearman's correlation between abundance of OTU259772 (*Lachnospiraceae*) from the ileal 16S dataset (see Supplementary Table 5) and RNA-Seq expression in ileal IECs of *Ror2, Fbp1, Tgfbr3, Acot12* and *Me1*. Circles represent individual mice and shaded bands indicate 95% confidence interval fitted by linear regression (**c**) Abundance of OTU259772 (*Lachnospiraceae*) by 16S sequencing and (**d**) abundance of *Anaerostipes caccae* by qPCR in ileal samples from healthy- and CMA-colonized mice. LD indicates samples that were below the limit of detection for the assay. (**e**) Spearman's correlation between abundance of OTU259772 (*Lachnospiraceae*) (16S sequencing) and abundance of *Anaerostipes caccae* (qPCR) in ileal samples from healthy- and CMA-colonized mice. Circles represent individual mice and shaded bands indicate 95%

confidence interval fitted by linear regression. Ileal samples that were above LD in both 16S and qPCR experiments are shown (n=19). (**f**) Expression of *Ror2, Fbp1, Tgfbr3, Acot12* and *Me1* in ileal IECs isolated from GF mice and from healthy- and CMA-colonized mice or mice monocolonized with *A. caccae* by qPCR. Data is normalized to *Hprt* as the housekeeping gene and shown as the fold change in expression from GF, set as 1. (**g**) Change in core body temperature at indicated timepoints following first challenge with BLG in BLG + CT sensitized CMA and *A. caccae*-monocolonized mice. (**h**) Serum BLG-specific IgE (**i**) BLG-specific IgG1 and (**j**) mMCPT-1 from mice in (**g**). (**k**) IL-13 and (**l**) IL-4 in culture supernatants of splenocytes from CMA or *A. caccae* colonized mice sacrificed 24h post challenge and stimulated for 72h with BLG. For **c**, **d**, **f**, **h, i, j**, **k**, **l** circles represent individual mice, bars represent mean+S.E.M. For **g**, circles represent mean, bars represent S.E.M. For **a-b**, n=18 (healthy) or 18 (CMA) mice per group. For **c-d**, n=19 (healthy) or 21 (CMA) mice per group. For **f**, n=14 (GF), 20 (*A. caccae*), 18 (healthy) or 23 (CMA) mice per group. For **g-j**, n=16 CMA and 16 *A. caccae* colonized mice pooled from three independent experiments with two different CMA donors (5 and 6), bars represent mean +S.E.M. For **k** and **l**, n=6 (CMA) and 9 (*A. caccae*) colonized mice from one experiment, circles represent individual mice, bars represent mean+S.E.M. DS-FDR method was used to compare groups in **c,** two-sided Student's *t*-test in **d,** one-way ANOVA with Bonferroni multiple testing correction in **f** or linear mixed-effect models in **g,** and two-sided Student's *t*-test in **h-l** after log transformation. $*P<0.05$, $**P<0.01$, $***P<0.001$.